AD NUMBER

AD911401

NEW LIMITATION CHANGE

TO

Approved for public release, distribution unlimited

FROM

Distribution authorized to U.S. Gov't. agencies only; Test and Evaluation; APR 1973. Other requests shall be referred to Rome Air Development Center, Attn: RBRN, Griffiss AFB, NY. 13441.

AUTHORITY

RADC USAF ltr, 27 Oct 1977

AD761 701

RADC-TR-73-105
Final Technical Report
April 1973

RELIABILITY OF THIN FILM NICHROME RESISTORS USED ON RADIATION HARDENED INTEGRATED CIRCUITS

Motorola, Incorporated

Rome Air Development Center
Air Force Systems Command
Griffiss Air Force Base, New York

RELIABILITY OF THIN FILM NICHROME RESISTORS USED ON RADIATION HARDENED INTEGRATED CIRCUITS

Wayne M. Paulson

Motorola, Incorporated

FOREWORD

This Final Report describes research by Motorola, Incorporated, Semiconductor Products Division, 5005 East McDowell Road, Phoenix, Arizona, under contract F30602-72-C-0069, Job Order Number 88090301. Sponsored by Rome Air Development Center, Griffiss Air Force Base, New York, the work was accomplished during the period 19 October 1971 to 19 June 1972.

Mr. Clyde H. Lane (RBRM) was the RADC Project Engineer. For Motorola Mr. K.V. Ravi was Project Leader and Mr. James T. Greener, Program Manager.

This technical report has been reviewed and is approved.

Approved:

D. F. BARBER
Chief, Reliability Branch
Reliability & Compatibility Division

Approved:

ALVIN P. HJORTEN, Lt Col, USAF
Assistant Chief
Reliability & Compatibility Division

FOR THE COMMANDER:

CARLO P. CROCETTI
Chief, Plans Office

ABSTRACT

The effects of corrosion, oxidation and interdiffusion on the reliability of thin film Ni-Cr resistors were studied. These properties were found to depend upon the composition and thickness of the films. The Ni-Cr thin films were found to be corrosion-resistant to salt solutions and to most acids with the exception of HF solutions and now Ni-Cr etches. From "water drop" tests it was found that unpassivated resistors are subject to anodic dissolution at potentials above 2.5V. The Al metallization also dissolves at potentials above 0.5V. Passivation with 10KÅ of SiO_2 protects the nichrome from anodic dissolution. The oxidation kinetics for 180 and 460Å films show an initial rapid increase in resistance followed by a slower diffusion-limited process. By comparison, the resistance for 800Å films remained nearly constant until after 8 hours at 500°C. The EBIC mode of the SEM revealed two phases in the films, so it was concluded that oxidation is a nonuniform process. Aluminum was observed to diffuse into the Ni-Cr resistors with an activation energy of 96kcal/mole. No discontinuities in resistance were observed for times up to 24 hours at 500°C.

EVALUATION

This report is an important contribution to the literature on nichrome thin film resistors. Nichrome films are widely used on radiation hardened circuits to eliminate photo currents associated with diffused resistor pn junctions. They are also being used as fusible links for programmable, read only memories. In both applications, the reliability of the film elements must be unquestioned. Our goal in this study was to isolate problems associated with nichrome resistors, define them with respect to cause, and eliminate the cause or assure that adequate safety factors are available, so that one may reasonably expect failure free operation over a five year period from screened parts. Motorola has demonstrated that such performance may be possible. The process and its exact control are the keys.

Motorola did a good job with the time available, providing a summary of known causes of failure, establishing limits for some mechanisms, and demonstrating the toughness of passivated resistors, fabricated according to good physical design principles, on a tightly controlled line. Some problems remain however. The behavior and significance of the packaging ambient was not discussed in the body of the report, we have no definite maximum limit of water vapor allowable in the package, and nothing appears in this report on the reliability of fusible links.

The highly accelerated test conducted on nichrome test patterns proved the capability of a good passivating glass to protect the film resistors. Water was detected in the packages, up to 1.4% of the residual atmosphere. Only 300 resistors were tested however and the glassivation process is still a variable one.

Clyde H. Lane

CLYDE H. LANE
Solid State Applications Section
Reliability Branch

TABLE OF CONTENTS

LIST OF ILLUSTRATIONS

LIST OF ILLUSTRATIONS (Cont'd.)

LIST OF ILLUSTRATIONS (Cont'd.)

LIST OF ILLUSTRATIONS (Cont'd.)

SECTION I

1.0 INTRODUCTION

The reliability of nichrome resistors is dependent upon understanding and controlling the materials and processes involved in their production. Motorola has acquired a large amount of experience with nichrome resistors. This has resulted in the highly reliable radiation hardened parts for the Minuteman II system being produced by Autonetics. Several aspects concerning the reliability of nichrome resistors using the Motorola process were reported by Philofsky, Stickney and Ravi[1]. They examined the structure of nichrome films, the formation of intermetallics with aluminum, electromigration and thermomechanical fatigue.

Other investigators have reported reliability problems associated with NiCr resistors. Using circuits from different manufacturers, Kapfer and Bart[2, 3] reported that the combination of water and bias was sufficient to cause nichrome resistor failures in circuits passivated with SiO. They further reported that temperature cycling from room temperature to -55°C resulted in resistor failures. Failures were also reported[4] for circuits with 100Å nichrome resistors with SiO passivation and sealed in Cerpacks. The problems were ascribed to moisture, carbon dioxide and bias.

The present investigation was undertaken in order to understand the factors involved in the reliability of nichrome resistors. The materials and processes required for the production of nichrome resistors include the following: (1) The composition and properties of the vapor-deposited thin films. (2) The aluminum deposition and resultant interface with the nichrome. (3) The photoresist, etchants and chemicals employed to delineate the resistors. (4) The passivation glass and its deposition process. (5) The package and sealing process. (6) The operating conditions for the device. In the present contract the corrosion character-

istics of nichrome were studied since it is a concern in both the processing and use. The oxidation of nichrome was examined because of the high temperature oxidizing atmospheres encountered during glass passivation and package sealing operations. The inter-diffusion of nichrome and aluminum was studied since an interface exists between the two metals. Temperature cycling tests were performed because of the reported effects on nichrome resistors.

SECTION II

2.0 Ni-Cr THIN FILMS

Thin films of nickel and chromium are used as stable resistor elements in microelectronic circuits, including radiation-hardened integrated circuits. These alloy films have sheet resistances on the order of several hundred ohms per square along with temperature coefficients of resistance (TCR) below 100 ppm/^{o}C. The properties of the Ni-Cr resistors will depend upon the composition, thickness and subsequent heat treatments. The phase diagram for Ni-Cr alloys[5] below 800^{o}C (Figure 1) shows a Ni-rich f.c.c. solid solution region for Ni compositions greater than 62% Ni. The remaining alloys consist of two phases: A Cr-rich b.c.c. phase and a Ni-rich f.c.c. phase. Figure 2 shows the effect of composition on the resistance and the TCR of Ni-Cr alloys[6]. The resistivity increases an order of magnitude across the solid solution region; it will then decrease linearly through the two-phase region[16]. Also, the TCR decreases with increasing Cr content. In addition, the Hall constant is negative for the Ni-rich solid solution alloys but becomes positive in the two-phase region[7].

The composition of the Ni-Cr resistors depends upon the method of deposition. The structure and properties of sputtered Cr-Ni films was reported by Mooij and deJong,[8] and Stern[9]. The present NiCr resistors are produced by vapor deposition. Therefore, the properties of the vapor-deposited resistors are dependent upon the various evaporation parameters such as the source composition and temperature, the vacuum, the deposition rate and the substrate. Since the vapor pressure of Cr is greater than that of Ni, Lakshmanan[10] found that the film composition changes from 38%Ni to 65%Ni with 15 sequential evaporations from an initially Cr-70%Ni source. The effects of film composition on the sheet resistance and TCR of evaporated nichrome films were reported by

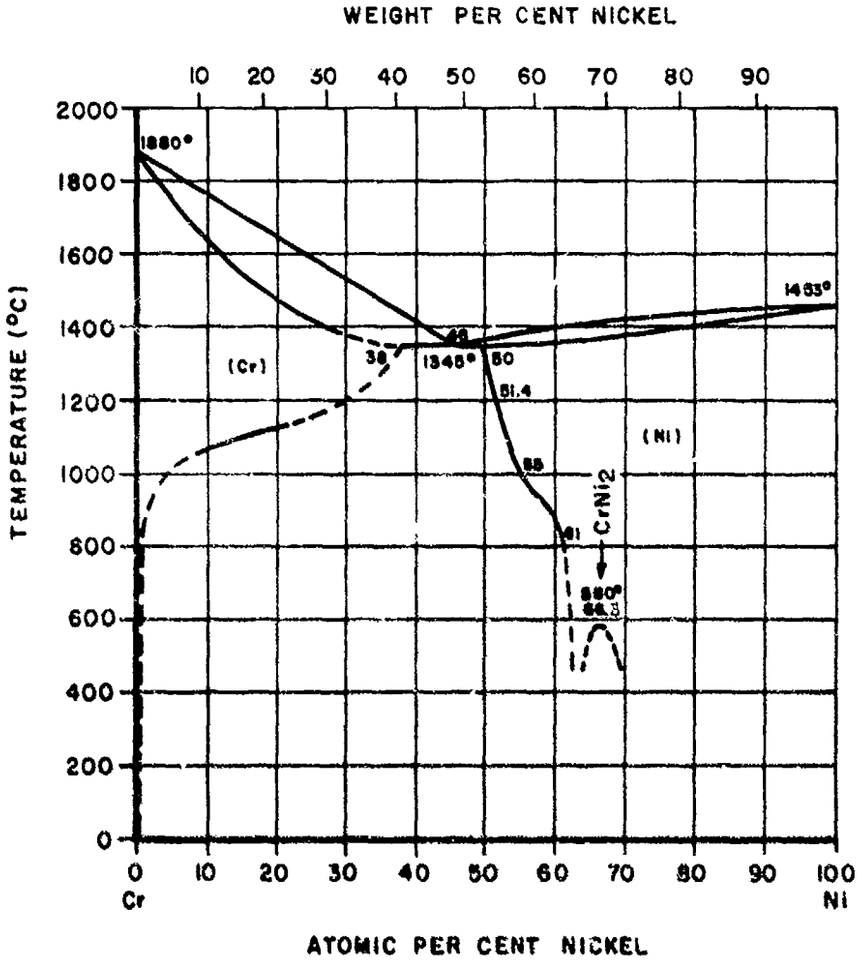

Figure 1. The Cr-Ni Phase Diagram[5]

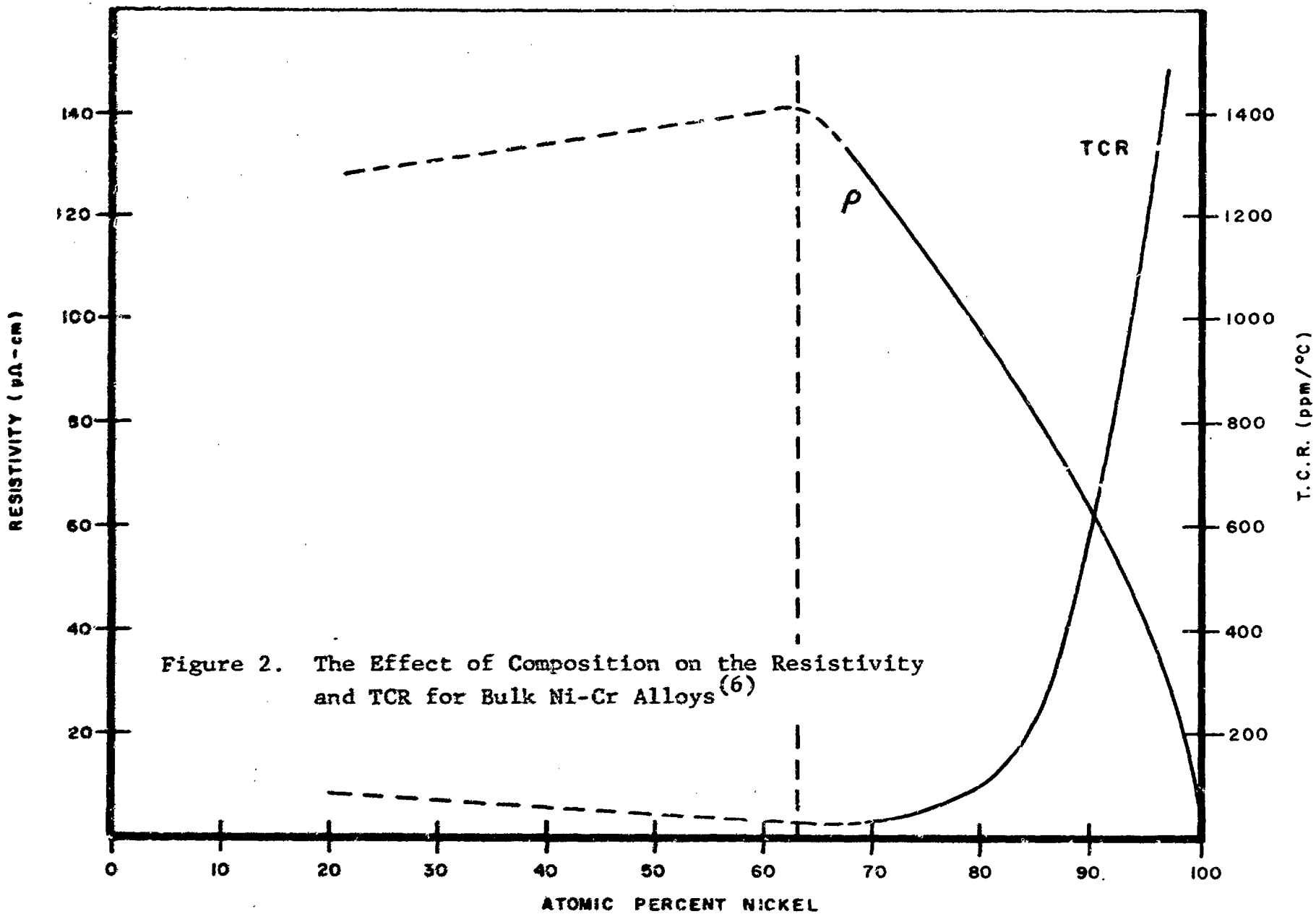

Figure 2. The Effect of Composition on the Resistivity and TCR for Bulk Ni-Cr Alloys[6]

Degenhart and Pratt[11], and Campbell and Hendry[12]. The later investigators found that at 100 ohms/sq. the TCR was approximately 200 ppm/°C at 80% Ni while only 30 ppm/°C at 30% Ni. The substrates also affect the structure and properties of the nichrome films. Voids were seen in 150Å films deposited on rock salt[13] and 200Å films on noncorrosive glass were nonconductive[14]. In contrast, 150Å NiCr films deposited on thermal SiO_2 were free of any voids or porosity[1]. Further information concerning Ni-Cr thin films is given in recent review articles by Maissel[15], Berry, Hall and Harris[16], Schwartz and Berry[17] and Dummer[18].

Since the deposition parameters affect the film composition, structure and resulting electrical properties, they are important considerations in the production of reliable nichrome resistors. The present resistors are deposited by an electron beam evaporator using a Ni-30% Cr source. The composition of the resulting films was Ni-70% Cr, as determined by microprobe analysis. Substrates of thermal SiO_2 were used at a substrate temperature of 300°C. Both the resistivity and the TCR are dependent upon the film thickness. Figure 3 shows the linear plots of resistance versus temperature for 180 and 460Å NiCr films, giving temperature coefficients of 95 and 182 ppm/°C, respectively. Vacuum annealing increased the TCR from 182 to 344 ppm/°C for the 460Å NiCr. Aging the NiCr resistors in an oxygen atmosphere increases the resistance and decreases the TCR. Figure 4 shows the changes in the resistance and TCR for a 180Å NiCr film aged at 500°C in an oxygen atmosphere. The TCR decreases from 95 to 20 ppm/°C while the corresponding resistance increased by a factor of two. Similar effects of oxidation on the electrical properties would be observed by vapor depositing the NiCr in a poorer vacuum[19].

Therefore, the electrical properties of the Ni-Cr resistors depend upon the composition, thickness, deposition parameters and

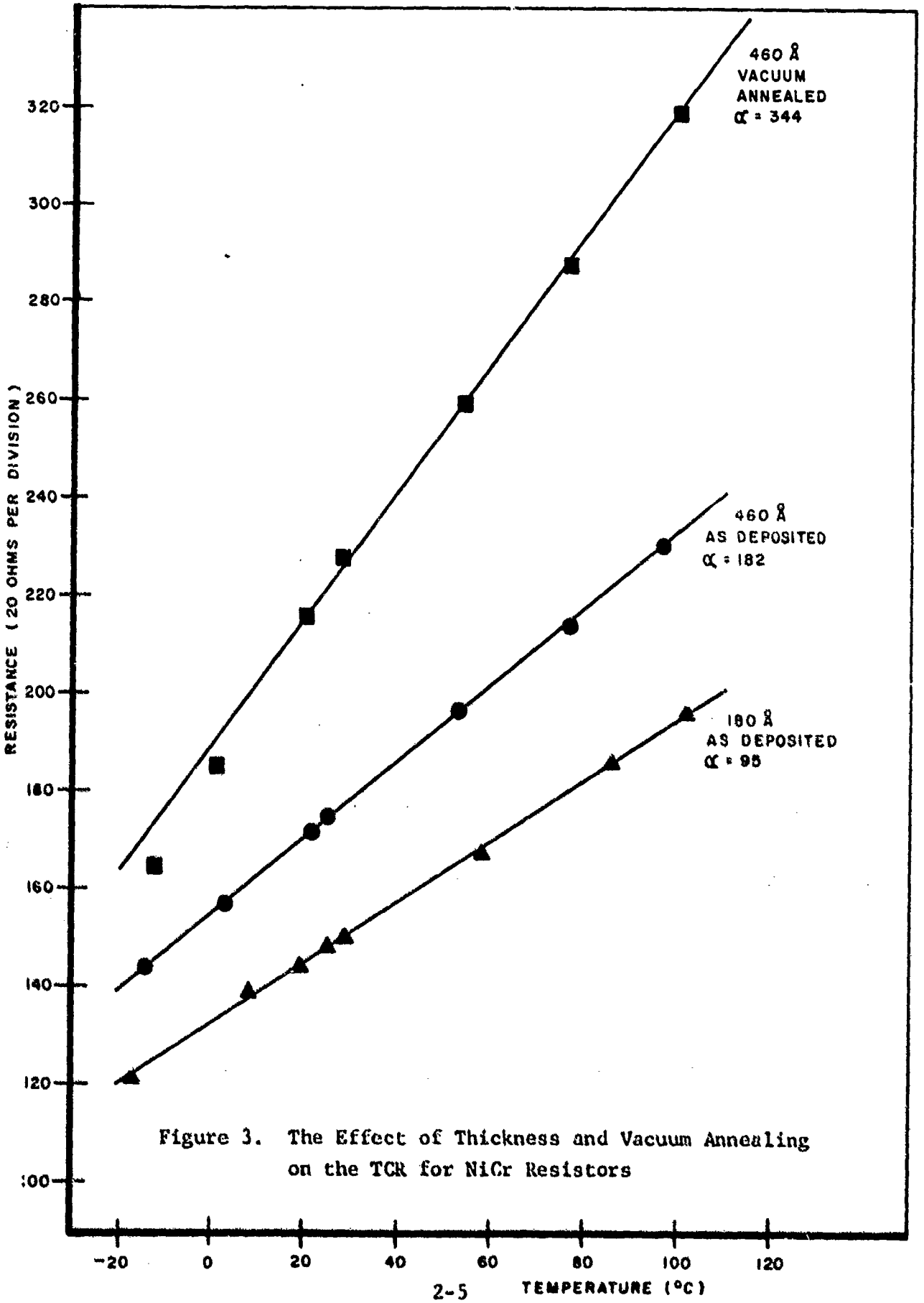

Figure 3. The Effect of Thickness and Vacuum Annealing on the TCR for NiCr Resistors

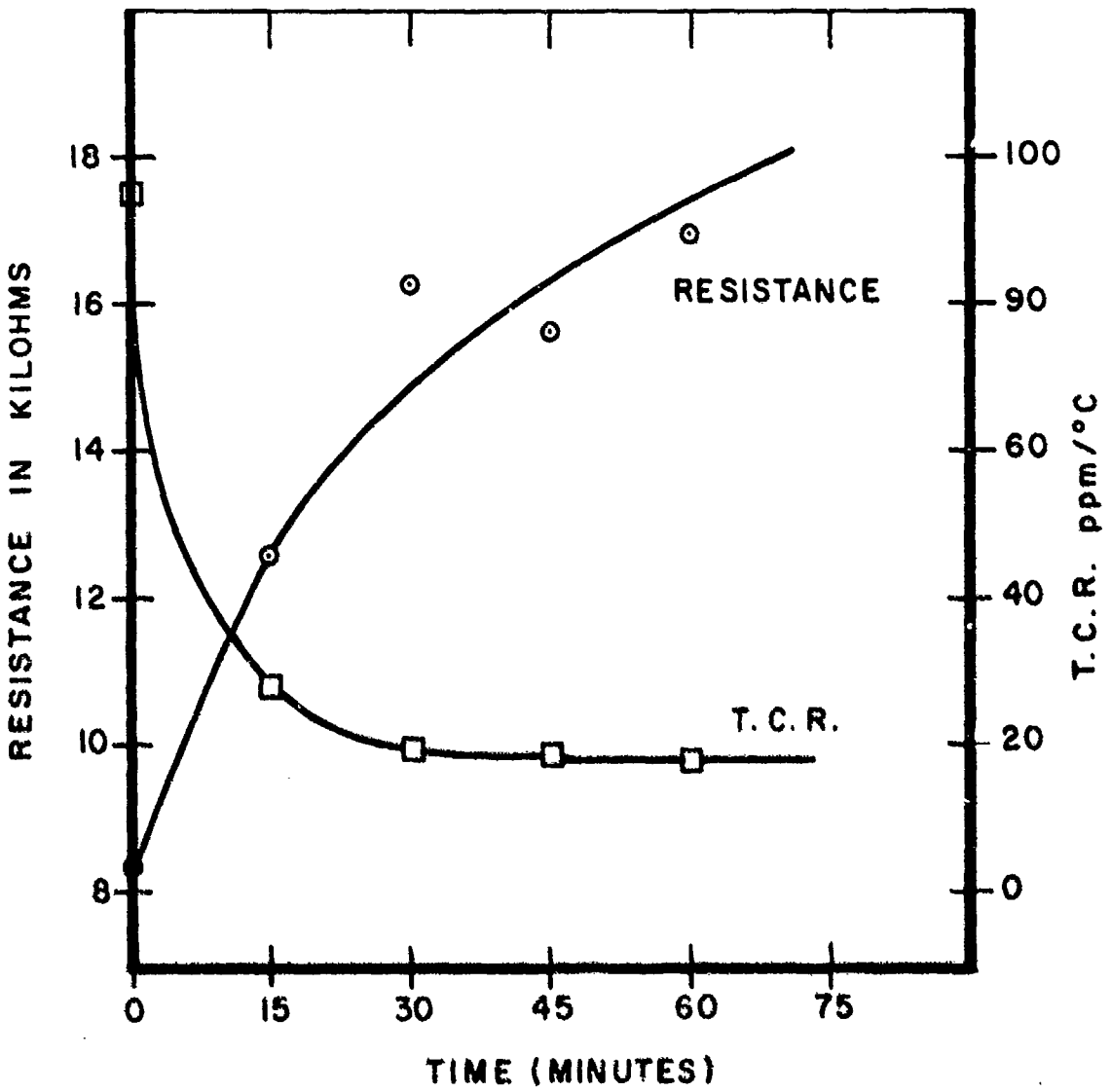

Figure 4. Changes in the Resistance and TCR Caused by Aging NiCr Resistors at 500°C in an Oxygen Atmosphere

subsequent heat treatments. These variables must be understood and controlled in order to produce reliable nichrome resistors. Throughout this report the use of "nichrome (NiCr) resistors" will refer to the composition Ni-70% Cr. The results obtained in the present report may not apply to Ni-Cr resistors with different compositions.

SECTION III

3.0 CORROSION

One aspect of the reliability of nichrome resistors concerns the solutions and atmospheres to which the nichrome is exposed during and after processing. For this reason, the corrosion of nichrome was examined. This section first presents a general discussion of corrosion and the factors of importance in corrosion processes. The experimental results are then presented and discussed.

The basic requirements for corrosion are two electrodes, an interconnecting solution and a driving force. The driving force arises from either a difference in the chemical potentials of two elements or from an external applied voltage. There will be two reactions occurring simultaneously--one at the anode and the other at the cathode. The anodic reaction is of the form

$$M \rightarrow M^{+z} + Ze^{-} \tag{1}$$

while the cathodic reaction is of the form

$$X + e^{-} \rightarrow X^{-}. \tag{2}$$

The cathodic reactions are of most importance in electroplating. In aqueous corrosion, the most common cathodic reactions[20] are the reduction of hydrogen

$$2H^{+} + 2e^{-} \rightarrow H_2(g),\ E_o = 0.0 \tag{3}$$

and the reduction of oxygen

$$O_2 + 2H_2O + 4e^{-} \rightarrow 4OH^{-},\ E_o = +0.401. \tag{4}$$

The anodic reactions are of most concern for corrosion since these involve metal dissolution. The corrosion potentials, E, are measured relative to the standard hydrogen electrode. By this

means the electrochemical series is obtained and is readily available[21]. From the electrochemical series one can predict the thermodynamic possibility of a particular reaction; however, it does not provide any kinetic information. The potentials are related to the concentration and pH of the solution by means of the Nernst equation

$$E = E^{o} + (RT/F)\ \ln\ (\text{products/reactants}), \qquad (5)$$

where E^{o} is the standard potential, R the gas constant, T the absolute temperature, and F the Faraday constant. For example, the potential of the reaction[21]

$$Cr_2O_3 + 5H_2O = 2CrO_4^{=} + 10H^{+} + 6e^{-} \qquad (6)$$

is given by

$$E_o = + 1.386 - 0.098\ pH + 0.0197\ \log(CrO_4^{=}). \qquad (7)$$

Figure 5 shows a corrosion cell with two electrodes that are connected by a resistor. A plot of the potential at each electrode versus the current is shown schematically in Figure 6. With an open external circuit the corrosion potentials of the anode and cathode are E_m and E_x. As the resistance is decreased the potentials approach a common value E_{corr} and the corresponding current I_{corr} indicated in the diagram. The corrosion rate is proportional to I_{corr} while the intensity of the corrosion is proportional to I_{corr}/anode area.

The corrosion of metals is affected by numerous factors. One factor is the metal or metals that form the corrosion cell. The anodic metal determines the potential difference available to drive the reaction while the cathodic metal and its surface affect the kinetics of the cathodic reaction (equation 3). A second

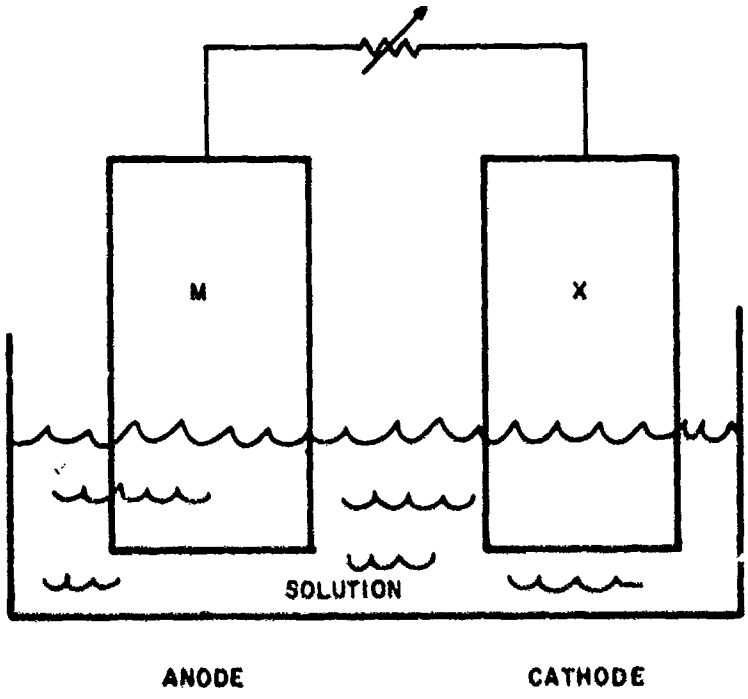

Figure 5. A Corrosion Cell Which Consists of an Interconnected Anode and Cathode in a Solution

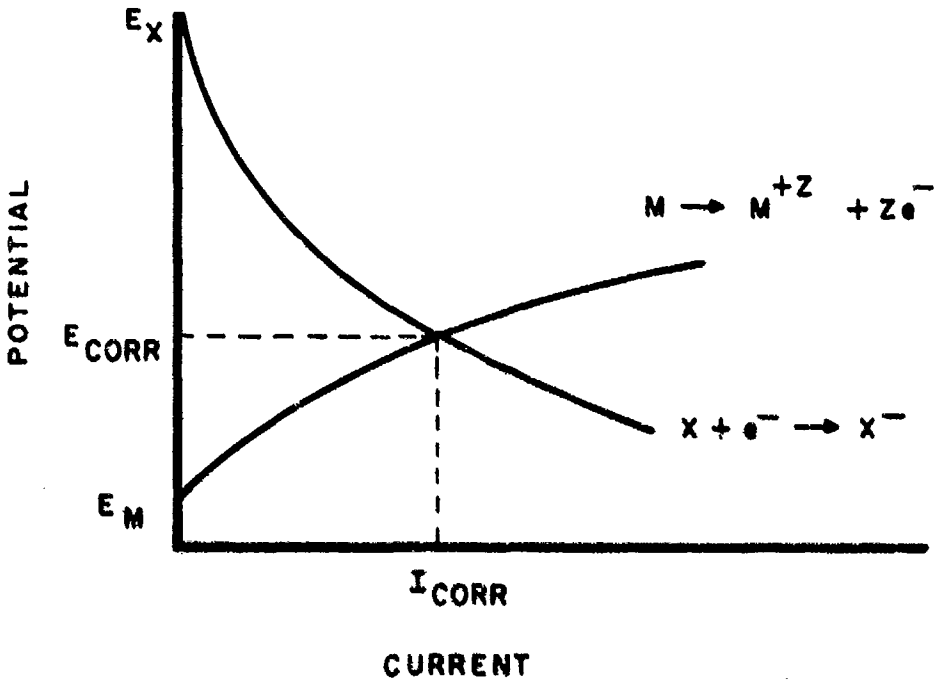

Figure 6. Graph Showing Current vs the Potential[20] for the Corrosion Cell in Figure 1

factor is the driving force for corrosion. An external driving force can raise the corrosion potential (Figure 6), resulting in accelerated corrosion. A third factor concerns the properties of the solution such as the conductivity, the pH, the concentration of ions (M^{+z}), dissolved gases (O_2), and complexing agents such as Cl, CN or NH_3. The surface of the metal is a fourth factor. This includes dislocations, grain boundaries and oxide films. A fifth factor is the relative areas of the anode and cathode which may provide a limiting reaction in the corrosion process.

The effects of some of these variables can be seen graphically in Pourbaix diagrams[21]. These diagrams plot the potential as a function of pH. Figures 7, 8 and 9 show the diagrams for Ni, Cr and Al, respectively. The dotted lines labeled (a) and (b) represent the reactions $H_2 = 2H^+ + 2e^-$ and $2H_2O = O_2 + 4H^+ + 4e^-$ so that between these boundaries water is stable. From the Pourbaix diagrams it can be seen that the metals Ni, Cr and Al are thermodynamically unstable in neutral solutions; however, they form surface oxides which stablize the metals. From the diagrams it can be seen that Al corrodes in both acidic and basic solutions. On the other hand, both Ni and Cr form stable oxides in neutral and basic solutions, but are corroded in acid solutions. It is further evident that at sufficiently high voltages, both Ni and Cr are subject to corrosion. The Pourbaix diagrams are therefore useful in predicting corrosion behavior.

In the present work, two types of corrosion experiments have been performed. The first set of experiments concerned the effect of chemicals on the NiCr resistors. The second set of experiments involved the effects of water and bias on the NiCr resistors. First, the chemical corrosion experiments will be discussed. This will be followed by the results from the "water drop" tests.

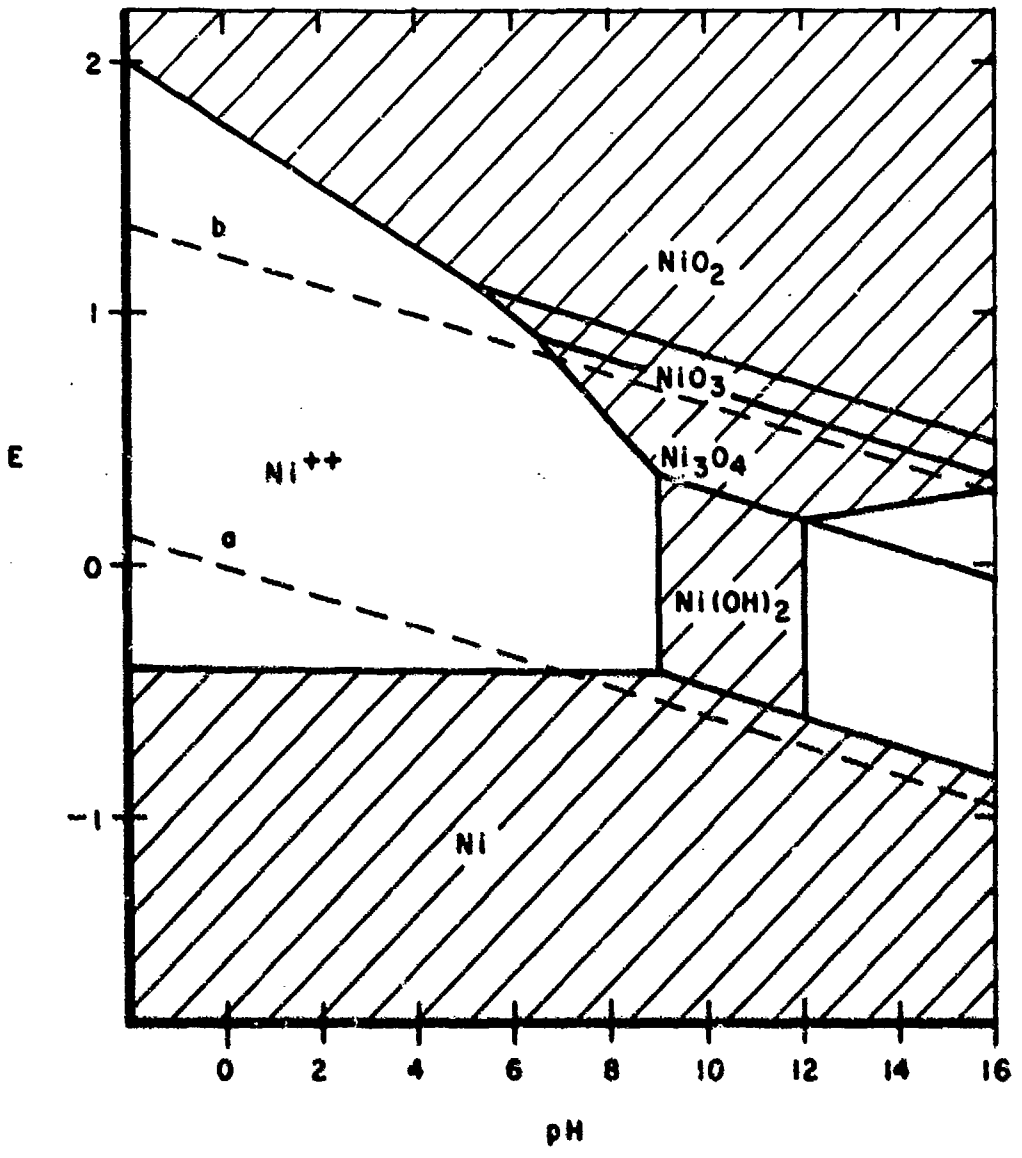

Figure 7. Pourbaix Diagram for Nickel[21]. The hatched areas indicate immunity and passivation domains. The un-hatched areas indicate corrosion domains.

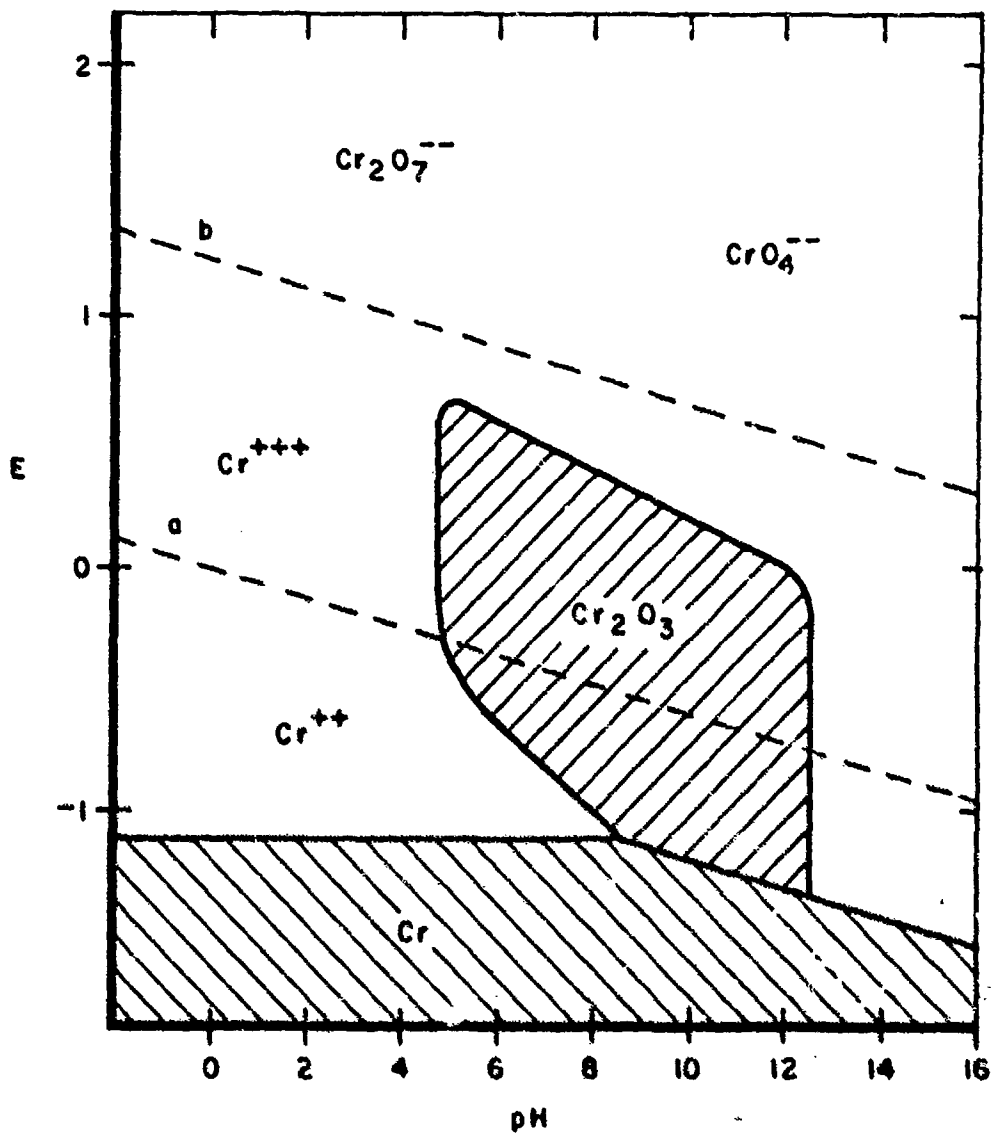

Figure 8. Pourbaix Diagram for Chromium[21]

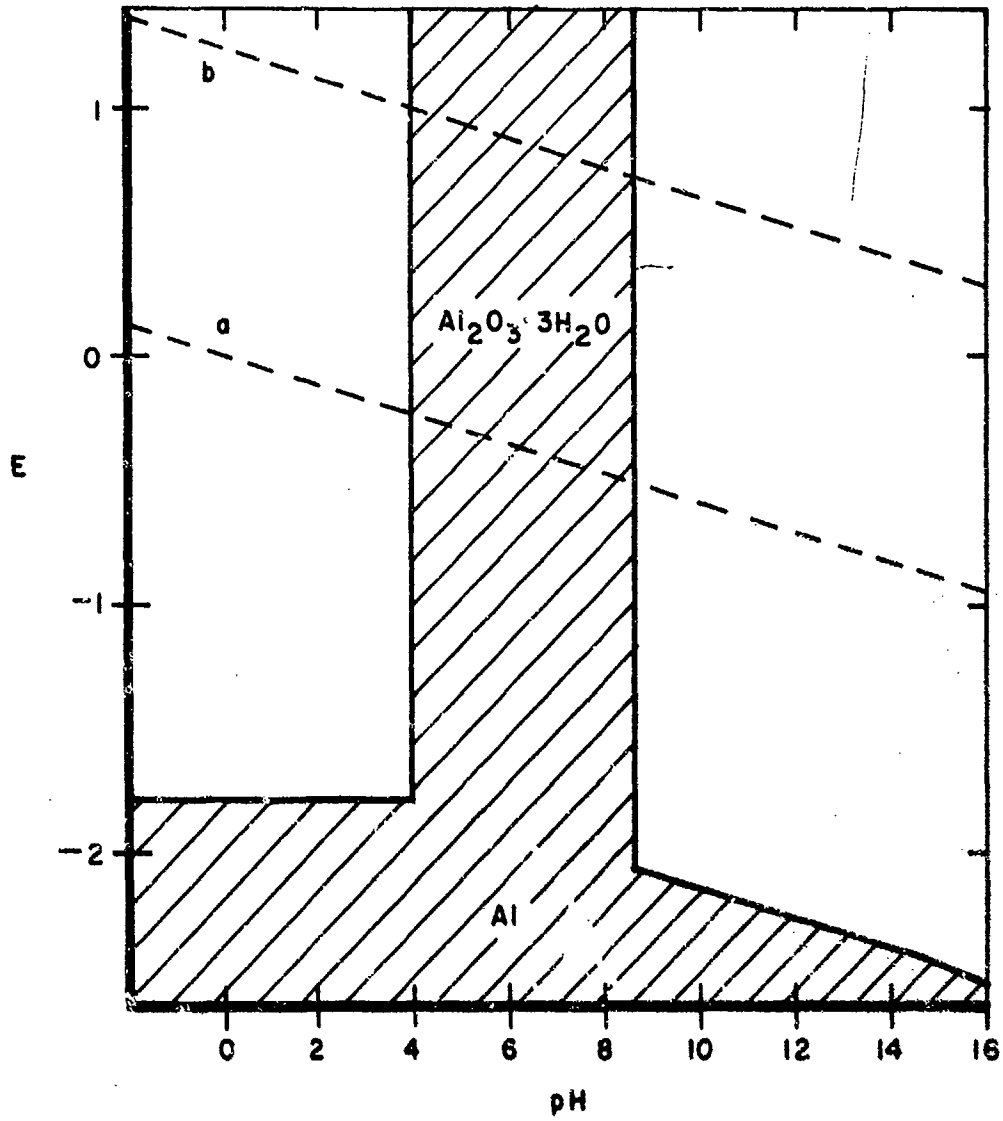

Figure 9. Pourbaix Diagram for Aluminum[21]

For the chemical corrosion experiments, both NiCr thin films and NiCr resistors with Al metallization, were immersed in different solutions to determine the conditions under which NiCr is subject to corrosion. These specimens were then periodically examined microscopically for evidence of corrosion. Particular emphasis was placed on the solutions that the NiCr encounters during processing; also salt solutions were studied since the Cl^- ion has a detrimental effect on corrosion. Table I lists the solutions and temperatures that were examined along with the corrosion results. The listed times indicate the maximum exposure to a particular solution. The first 10 solutions were acids and only the NiCr etches, the HF solutions, and the combination of HNO_3 - HCl were observed to attack NiCr. The Fe Cl_3 pits the NiCr but no general dissolution occurred. The dilute HF solution etches small holes at random in the NiCr (Figure 10). Circuits that were passivated with SiO_2 were also exposed to the HF. The HF dissolves the SiO_2 and then attacks the NiCr as shown in Figure 11. Again there is some random attack of the NiCr but the etch has completely opened the NiCr resistors at the Al-NiCr interface.

The corrosive effects of the resist stripper J-100 have been described by Glang and Gregor[22]. The J-100 contains tetrachloroethylene, dichlorobenzene and phenol, and reacts acidicly. Nichrome is quite resistant to J-100 and even J-100 plus water. However, when both Al and NiCr are present the J-100 plus water will attack the Al and subsequently react with the NiCr. Thus, the NiCr-Al interface is particularily susceptable as shown in Figure 12. It is assumed that the J-100 forms chlorides with the Al which subsequently react with the NiCr.

The corrosive effects of NaCl and KCl solutions were examined in order to observe the effect of the chloride ion on the corrosion of NiCr. As shown in Figure 13 the NiCr was pitted by both salt solutions but no general attack was observed. Large regions of the Al metallization were completely corroded by the salt solutions (Figure 13).

TABLE I

Solution	Temperature	NiCr	NiCr and Al
Conc. HNO_3	R.T.	No Attack 1 hr.	No Attack 1 hr.
Conc. HCl	R.T.	No Attack 1 hr.	No Attack 1 hr.
1-HCl 1-H_2O	R.T.	No Attack	No Attack
1-HNO_3 1-HCl 1-H_2O	R.T.	Slowly Dissolves 1 hr.	Al Dissolves 5 min, NiCr Slowly Dissolves
1-HF 10-H_2O	R.T.	Spotty Dissolution 10 min.	Slowly Etches Al and NiCr
Solution B (H_3PO_4, HNO_3 and H_2O	R.T.	No Attack	Al Dissolves 1 hr.
Solution B	70°C	No Attack 90 min.	Al Dissolves 30 sec.
Ce $(SO_4)_2$ (NiCr etch)	60°C	Dissolves < 1 min.	Al and NiCr Dissolve Slowly
$(NH_3)_2Ce(NO_3)_6$ (NiCr etch)	R.T.	Dissolves < 1 min.	Only attacks NiCr
Aqua Regia	R.T.	No attack 1 hr.	No attack 1 hr.
$FeCl_3$(1.4g/ec)	R.T.	Pits NiCr	Dissolves Al
J-100	105°C	No Attack 3 hr.	No Attack 3 hr.
J-100 + 5%H_2O	R.T.	No Attack 24 hr.	Attacks Both Al and NiCr
10% NaCl	R.T.	Pits NiCr	Dissolves Al
10% K Cl	R.T.	Pits NiCr	Dissolves Al

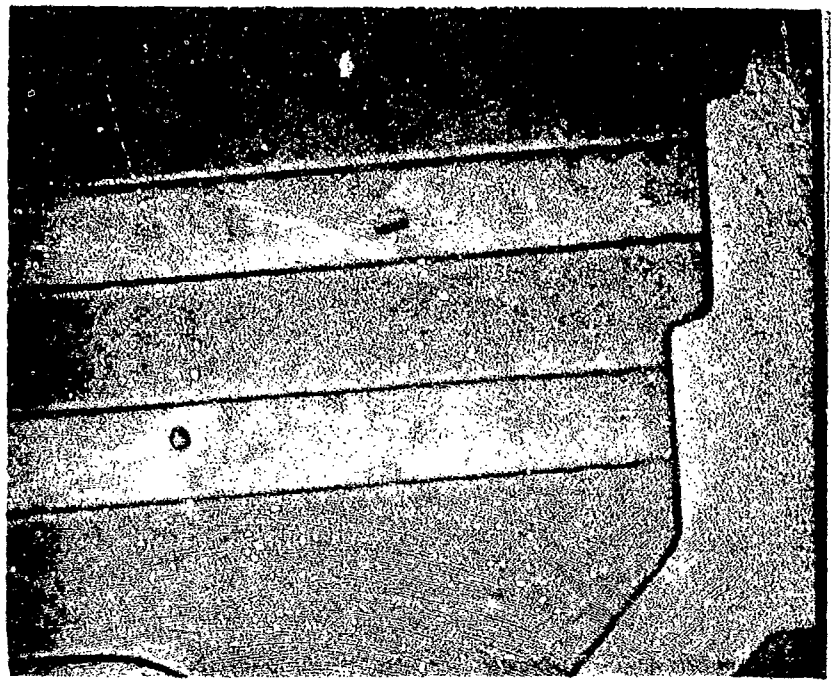

Figure 10. The Random Attack of a 10:1 HF Solution on Unpassivated NiCr

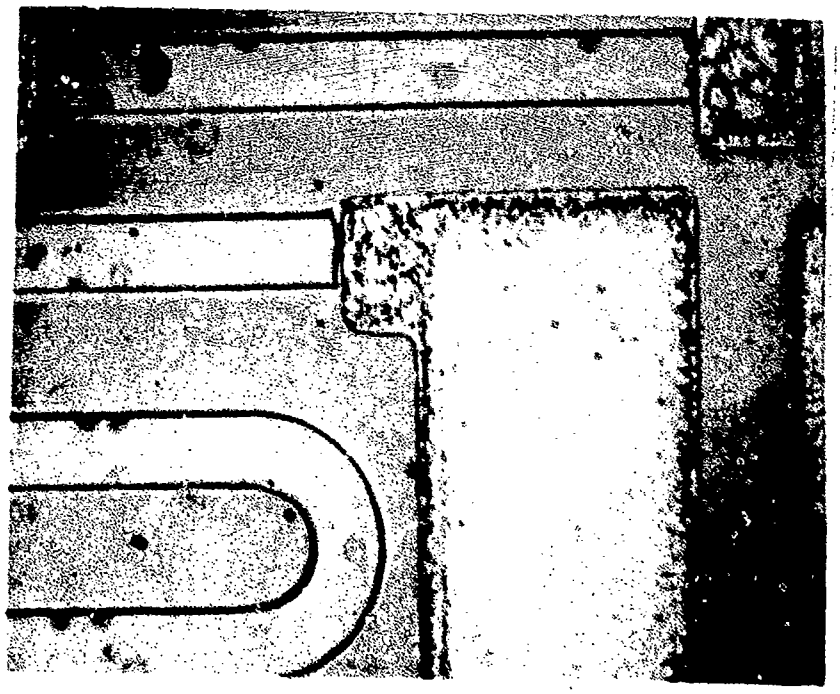

Figure 11. The 10:1 HF Solution Dissolves the SiO_2 Passivation and Then Attacks the NiCr. This attack is particularly severe at the Al-NiCr interface

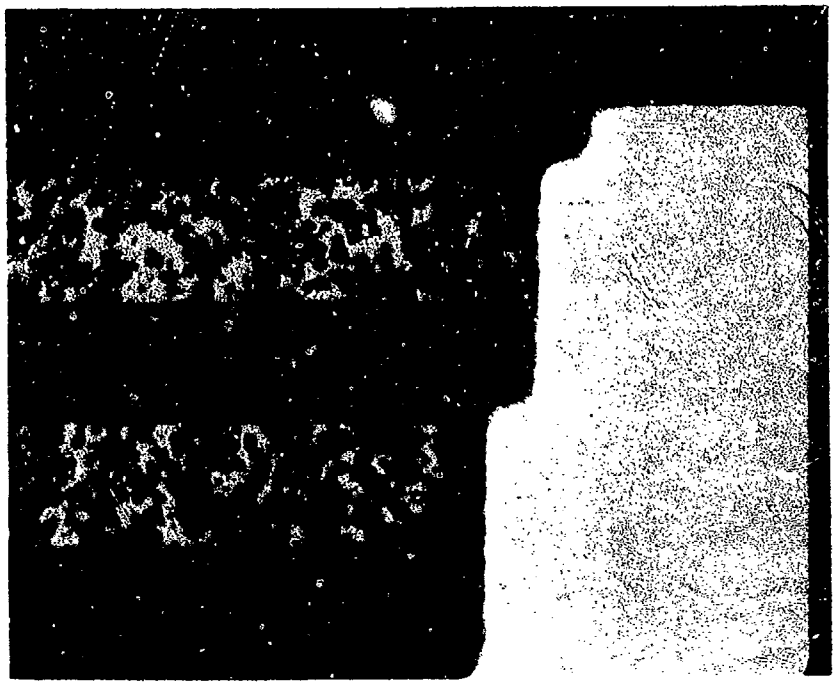

Figure 12. The Etching Effect of 5 Percent H_2O in J-100 on Circuits with NiCr Resistors and Al Metal. The attack is particularly intense at the interface.

Figure 13. The Pitting of NiCr and the Dissolution of Al Caused by a 24-hour Immersion in a 10-Percent KCl Solution

The second set of corrosion experiments are referred to as water drop tests. The experimental procedure was to place water on the circuits and then apply a voltage. One test structure consisted of two parallel NiCr resistors with Al bonding pads (Figure 14). A potential difference, V, between the resistors was applied by means of an external constant-voltage power supply. When the circuit was completely immersed in water, the following results were obtained. First, for $V > 2.5$ volts, both the Al and the NiCr dissolved at the anode (Figure 15). Second, for $0.5 < V < 2.5$ volts, only the Al dissolved (Figure 16). At potentials below 0.5 volt, no corrosion was observed. When water was only in contact with the NiCr, the same results were observed -- namely that NiCr dissolved from the anode for $V > 2.5$ volts while no dissolution occurred at lower voltages.

Water drop tests were also run using the 98 R test pattern. In this case, the voltage was applied across a single resistor stripe, which grounds the adjacent resistors. With water covering the circuit, only the Al dissolved, since it was at the highest potential (Figure 17). If the water is confined to the NiCr, then the NiCr dissolves at the edge of the water drop closest to the anode as shown in Figure 18. For this dissolution to occur there must be at least 2.5 volts between two resistors that are both connected by water.

Water drop tests were also run using a single NiCr resistor with a small water drop, as shown schematically in Figure 19. The voltage was slowly increased until dissolution was observed. When the potential drop across the water drop exceeded 2.5 volts, dissolution of the NiCr occurred along the edge of the water drop closest to the anode (Figure 20). As soon as the resistor develops an open circuit, the voltage across the gap increases which causes an increase in the dissolution rate. This dissolution continues towards the anode and is aided by the

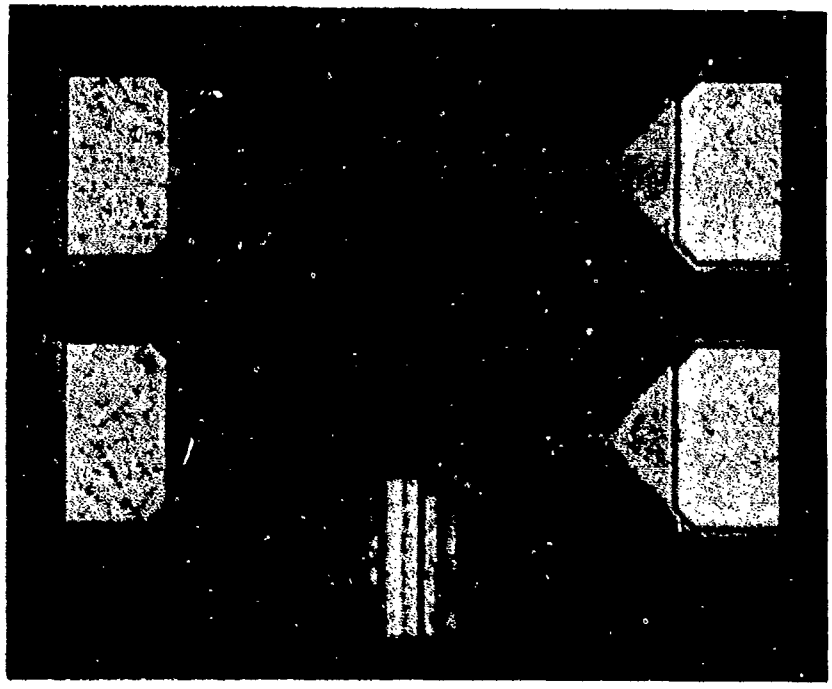

Figure 14. A Test Structure Used in the Water Drop Tests Which Consists of Two Parallel NiCr Resistors. (100X)

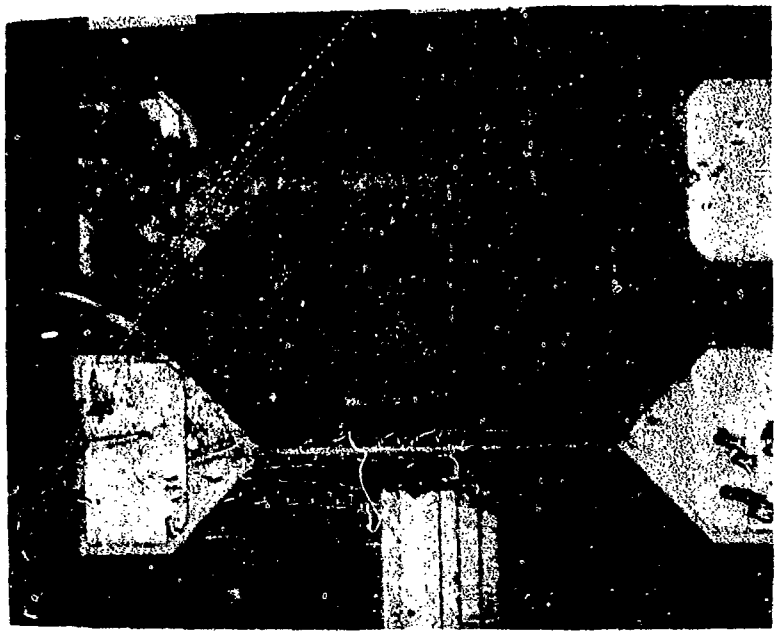

(+)

(-)

Figure 15. With a Potential Difference of 4 Volts, Both the Al and the NiCr Dissolve From the Anode When the Circuits were Immersed in Water

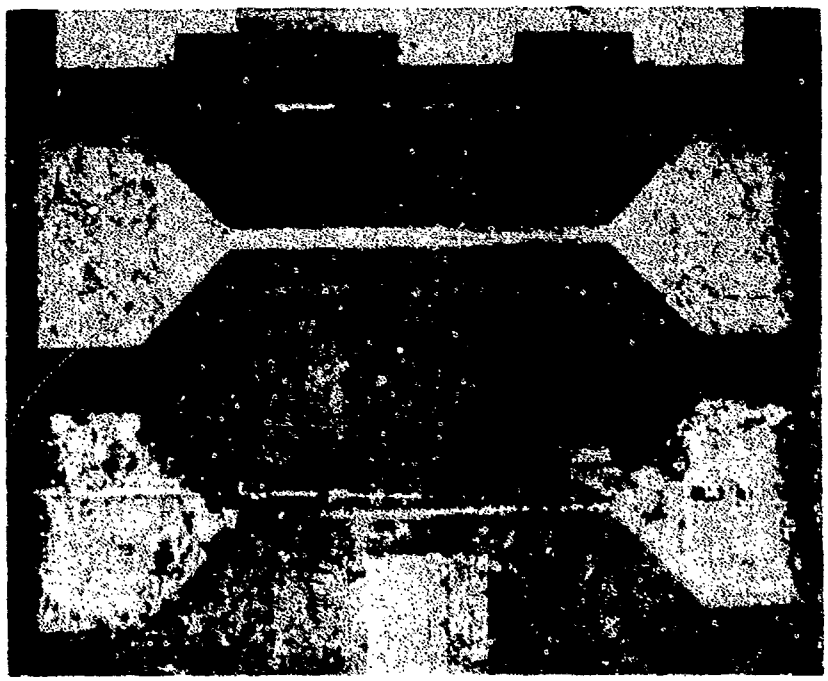

(+)

(-)

Figure 16. With a Potential Difference of 2.5 Volts, Only the Al Dissolves from the Anode and $Al(OH)_3$ collects at the Cathode When the Circuits were Immersed in Water

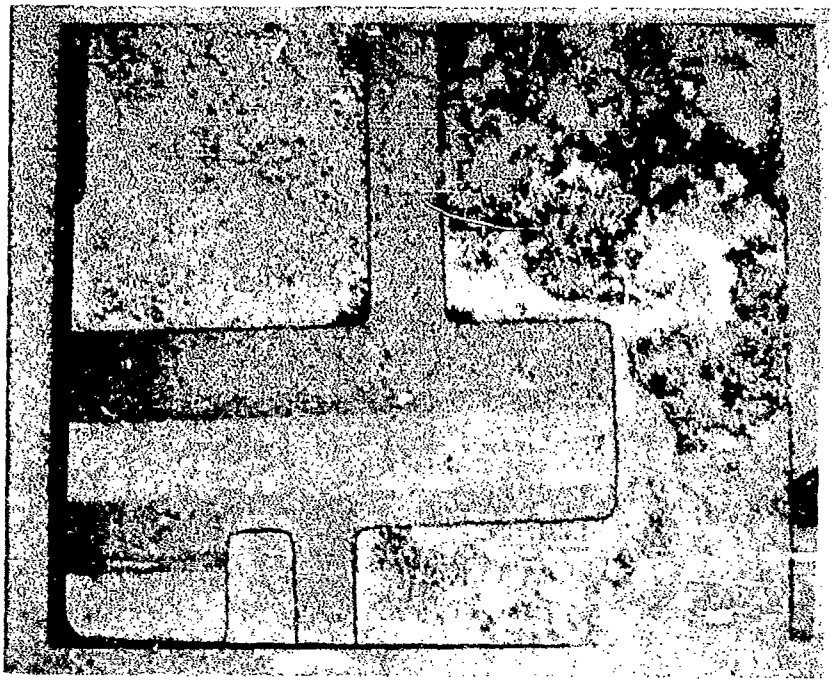

Figure 17. The Dissolution of Al at the Anode in the Immersion Water Drop Test at 5 Volts

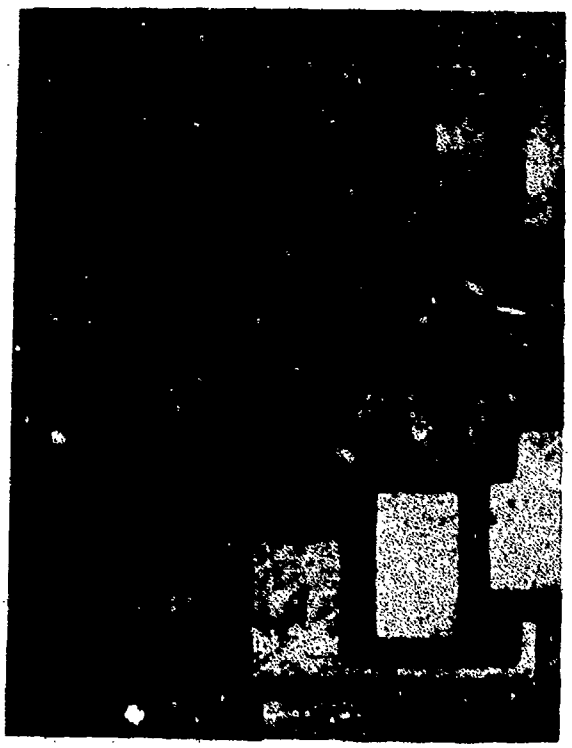

(-)

(+)

(-)

Figure 18. When Water Contacts only the NiCr, the NiCr Dissolves at the Edge of the Water Drop for Potential Differences Greater Than 2.5 Volts

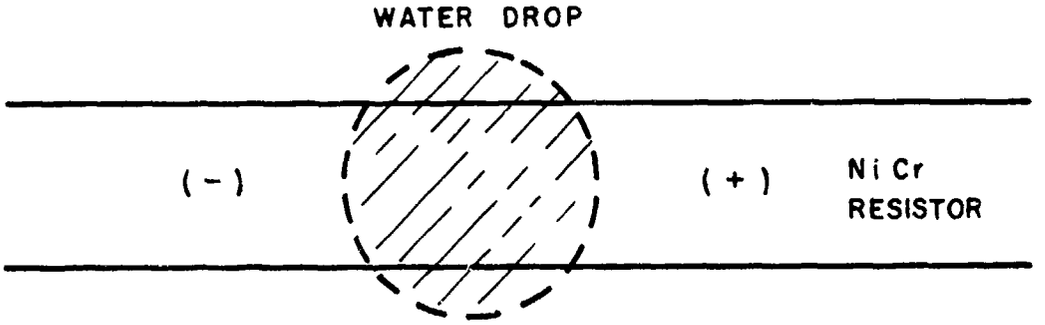

Figure 19. A Schematic of the Water Drop Test Using a Single NiCr Resistor

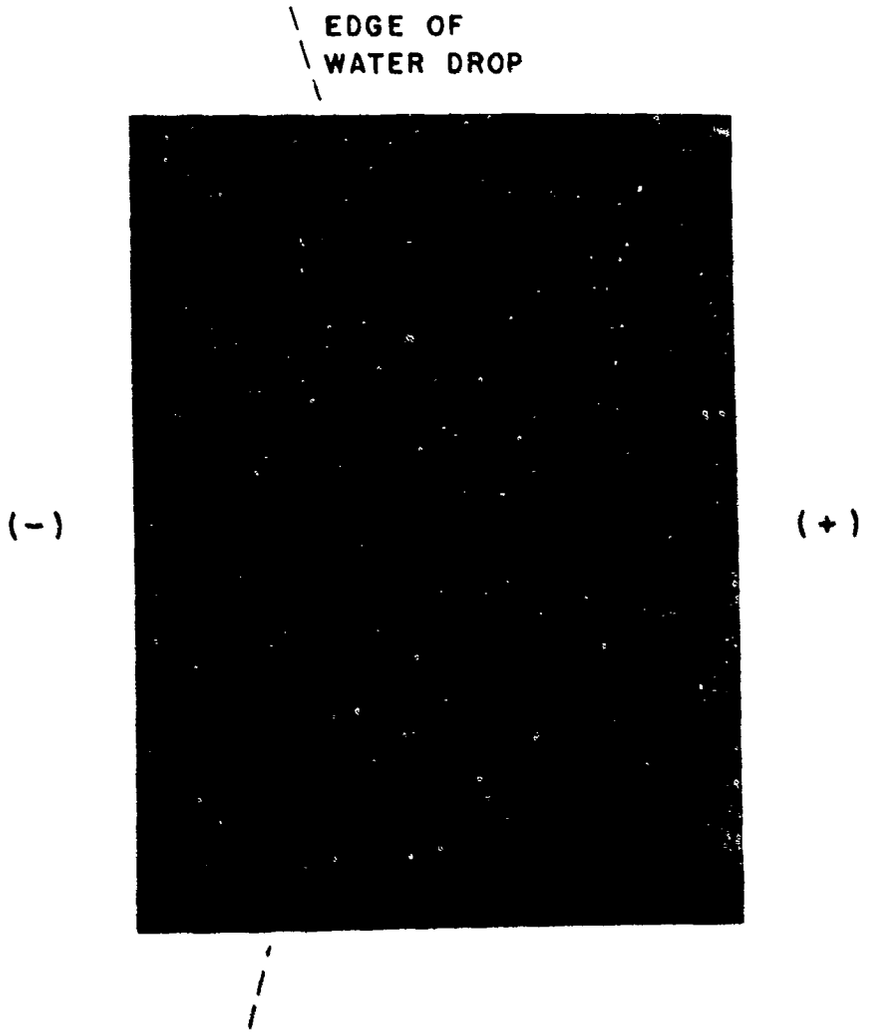

Figure 20. The Results of the Test Shown in Figure 15. Dissolution of the NiCr occurs when there is a potential difference of at least 2.5 volts across the water drop

fact that water wets the SiO_2. In this case, one side of the water drop is the anode and the other side is the cathode.

Water drop tests were also run using NiCr resistors that had been trimmed by oxidation. The resistors were still attacked at voltages above 2.5V, but the mechanism was different. In this case, the NiCr was converted to a insulating oxide as shown in Figure 21, and did not dissolve, as was observed with the as-deposited resistors.

The same water drop tests were repeated using circuits passivated with 10,000Å of SiO_2. When the circuits were immersed in water, the Al bonding pads rapidly dissolved. If the water were confined to the region above the NiCr resistors, no dissolution was observed. It was therefore concluded that the SiO_2 passivation is adequate to protect the NiCr from water. Similar results were obtained when using dielectrically-isolated, integrated circuits with NiCr resistors and Al metal. The results are shown in Figure 22 along with the voltages at each terminal. The Al dissolved rapidly at the positive terminals, while no corrosion of the NiCr was observed on these circuits.

The results of the water drop test illustrate the effects of the relative areas of the anode and cathode on corrosion. The corrosion rate of one metal can be accelerated by coupling it to a second more noble metal, especially if the area of the more base metal is smaller than that of the noble metal[20]. This situation is found with Al wire bonds on Au bonding pads. In dilute salt solutions, corrosion of the Al occurs most rapidly at the Au bonding pads on the package. In contrast, the Al metallization (large area) is more base than the NiCr resistor (small area), so that the Al may slow down the NiCr corrosion (Galvanic protection[20]). This was observed for the immersion water drop tests using the 98R circuits with unpassivated NiCr resistors.

Figure 21. The Results of the Water Drop Test on a Trimmed Resistor. The NiCr is further oxidized rather then dissolved at potentials above 2.5 V.

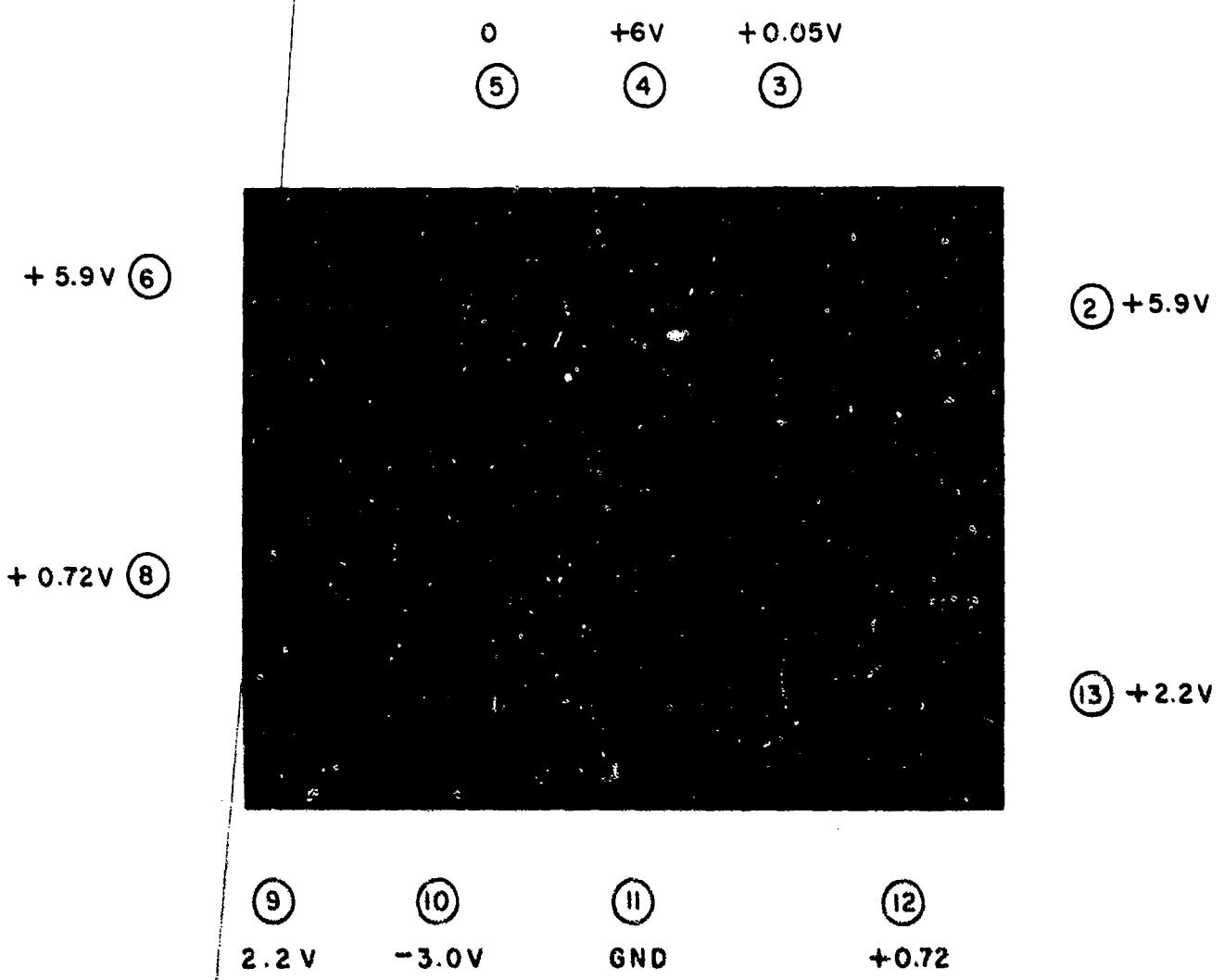

Figure 22. A Dielectrically Isolated Circuit After an Immersion Water Drop Test. The voltages at each terminal are shown. The Al dissolved from the positively biased bonding pads

The corrosion mechanism in these water drop tests is that of anodic dissolution. In all cases there is an anode and a cathode as was shown schematically in Figure 5. These can either be two different places on the circuit or the opposite sides of a single water drop. The driving force for this corrosion is the applied potential. The dissolution reactions[21] for pure Cr and Ni are

$$Cr = Cr^{+3} + 3e^-$$

$$E = -0.744 + 0.0197 \log (Cr^{+3})$$

and

$$Ni = Ni^{+2} + 2e^-$$

$$E = -0.250 + 0.0295 \log (Ni^{+2})$$

These reactions should occur spontaneously. However, since water by itself has no effect on NiCr, the equations of concern are as follows[21]:

$$Cr_2O_3 + 5H_2O = 2\ CrO_4^{=} + 10H^+ + 6e^-$$

$$E = +1.386 - 0.0985\ pH + 0.0197 \log (CrO_4^{=})$$

and

$$2\ NiO + H_2O = Ni_2O_3 + 2H^+ + 2e^-$$

$$E = +1.032 - 0.059\ pH$$

Since the potentials are positive for these reactions, a higher applied potential is required to drive the reactions to the right. The observed anodic dissolution of NiCr is consistent with the later two equations and could be predicted from the Pourbaix diagrams (Figures 7, 8 and 9). The corrosion of the Al occurs by

a different mechanism. Al_2O_3 is stable at nearly all potentials. However, at the anode the water decomposes and the local pH decreases. Thus, the solution becomes locally acidic and corrosion occurs. This reaction can be seen on the Pourbaix diagram (Figure 9), where the solution pH decreases and the solution can move outside the passivation region.

A summary of the corrosion experiments is as follows. The NiCr thin films are resistant to most acids except NiCr etches and the HF solutions; salt solutions result in the pitting of NiCr. Therefore, the NiCr thin films are quite corrosion resistant in agreement with the results observed for bulk nichrome[23]. The NiCr resistors are subject to anodic dissolution when there are two areas on a circuit that are connected by water and also have a potential difference of at least 2.5 volts. Therefore, the NiCr thin films should be protected from moisture, as is also required for bulk NiCr resistors[16, 18]. The present experiments show that 10,000Å of SiO_2 passivation glass provides adequate corrosion protection for the NiCr.

SECTION IV

4.0 OXIDATION

The oxidation characteristics of NiCr are an important consideration for the reliability of nichrome resistors, since they are exposed to oxidizing atmospheres during processing. The resistors are trimmed by heating in air. Furthermore, oxidizing atmospheres are encountered during the glass passivation and package sealing processes. For these reasons the oxidation of NiCr films was examined to understand the mechanisms and to determine the kinetics of oxidation.

The experimental procedure was to measure the resistance at room temperature and then to oxidize the NiCr at fixed temperatures for different time intervals. For 180Å films of Ni-70% Cr, the resistance ratio R/Ro, where Ro is the initial resistance, is plotted as a function of time at 400, 450, 475 and 500°C in Figure 23. These plots show an initial rapid increase of approximately 20 percent at all temperatures. At 400°C the resistance increases to a maximum after approximately 3 hours and then begins to decrease. For times longer than 8 hours, the resistance again increases and after 15 hours at 400°C R/Ro is 1.54. At 450 and 475°C the resistance continues to increase up to a maximum annealing time of 8 hours. At 500°C R/Ro increases to a value of 2, where it levels off for a short time and then increases rapidly again. After 3 hours at 500°C more than 50 percent of the resistors were no longer conducting. The error bars shown in these plots indicate the range of values for eight different resistors on a single chip. The largest changes occurred for the more narrow resistors (0.36 mil) while the smallest changes occurred for the wider resistors (1 mil).

The oxidation kinetics were also determined at 500°C for NiCr films of 180, 460 and 800Å and are shown in Figure 24. R/Ro is nearly constant until after 2 hours when it again increases

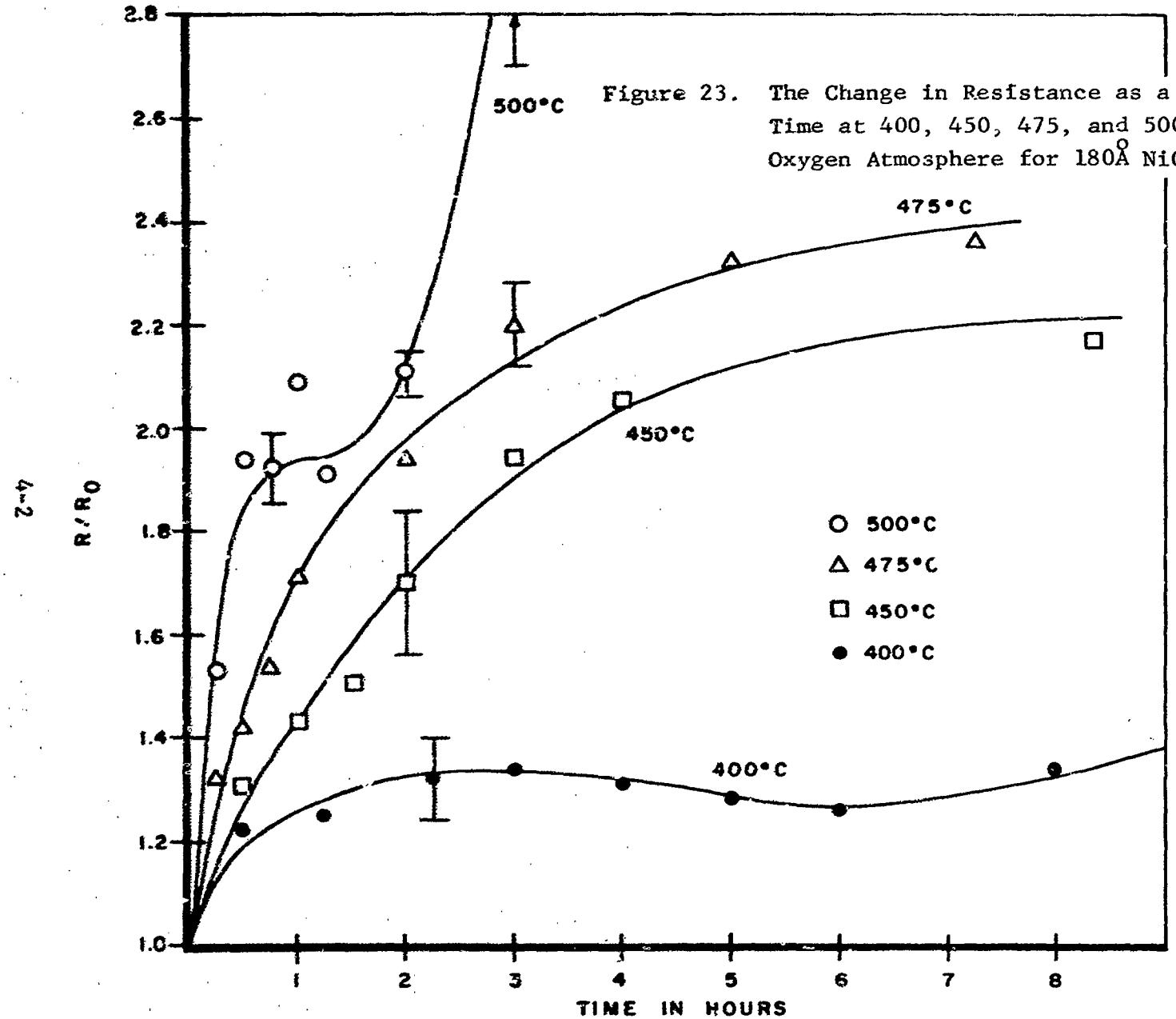

Figure 23. The Change in Resistance as a Function of Time at 400, 450, 475, and 500°C in an Oxygen Atmosphere for 180Å NiCr

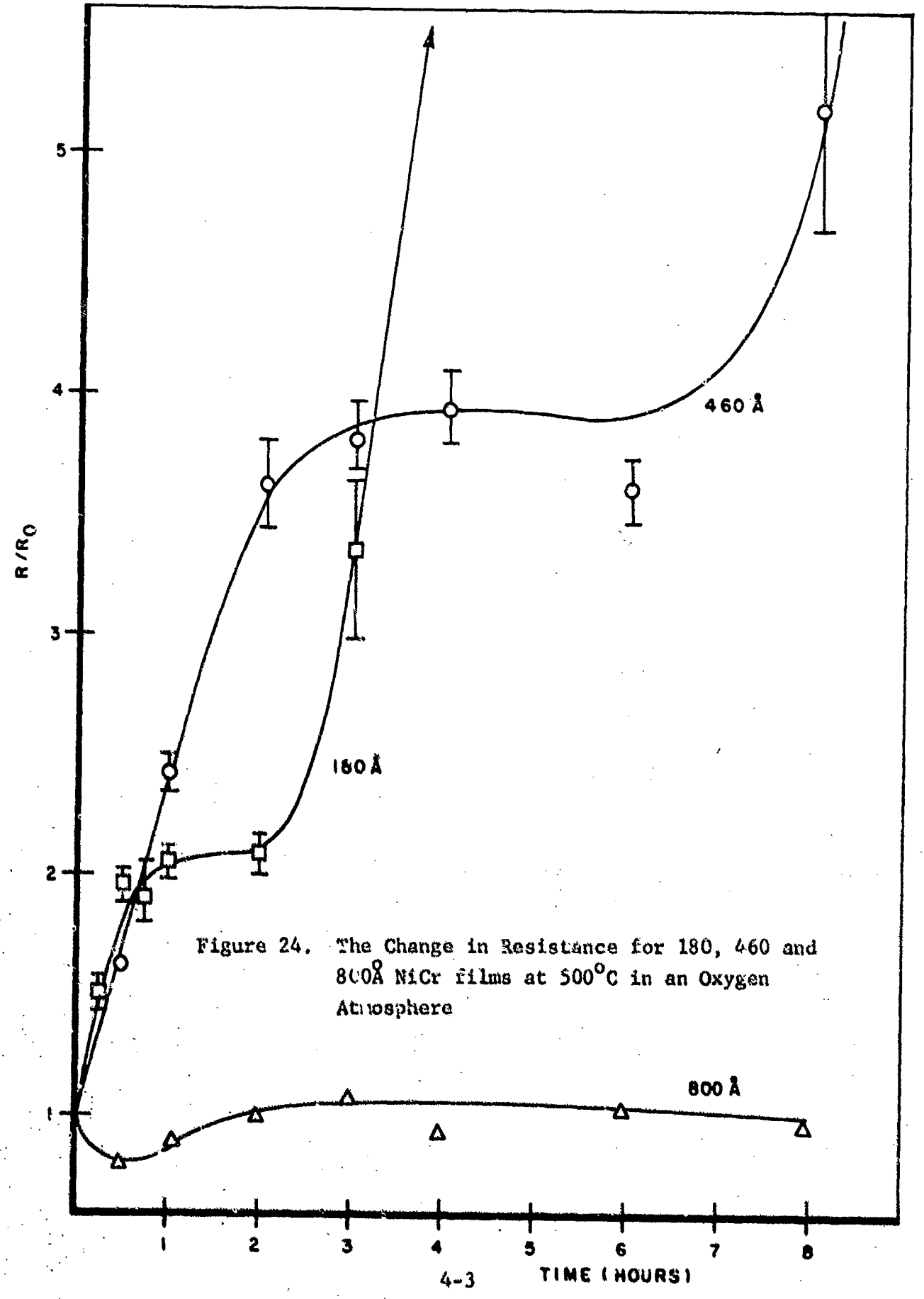

Figure 24. The Change in Resistance for 180, 460 and 800Å NiCr films at 500°C in an Oxygen Atmosphere

rapidly. The films were completely oxidized after 4 hours. For the 460Å film the shape of the curve is similar to that for the 180Å film; however, the ratio R/R_o increases to a plateau at approximately 3.9. For times greater than 8 hours, the films were completely oxidized. The resistance behavior of the 800Å NiCr films is quite different. The resistance initially decreases approximately 25 percent within 30 minutes. The resistance then increases to its original value and remains nearly constant for approximately 10 hours. For oxidation times greater than 10 hours the resistance increases as shown in Figure 25. The films were still conducting after 24 hours at 500°C but considerable interdiffusion had occurred. This diffusion of the Al into the NiCr is discussed in detail in the next section. In contrast to the increase in resistance caused by the oxidation, the vacuum annealing of NiCr resistors lowers the resistivity. For example, the resistance decreases 25 percent after 3 hours at 500°C.

When the oxidized NiCr resistors were microscopically observed, small spots were observed which indicated nonuniform oxidation (Figure 26). For this reason the NiCr resistors were observed in the SEM using the electron beam induced current (EBIC) mode[24]. By this technique the film is examined in transmission and differences in the product of density times thickness (ρX) can be seen, where ρ is the density and X is the thickness. Figure 27 shows a secondary electron image of a NiCr resistor with Al bonding pads. The same region is shown in Figure 28 using the EBIC mode. A NiCr resistor in the as-deposited condition is seen in Figure 29, where little contrast is apparent. By comparison, two phases were observed in a NiCr resistor that was oxidized for 1 hour at 500°C (Figure 30). Another resistor was oxidized for 6 hours at 490°C in order to more closely observe the two-phase structure. This specimen is shown in Figures 31 and 32 at magnifications of 7000 and 22,000, respectively. They reveal a dark matrix with light particles between 1000 and 5000Å in diameter. No

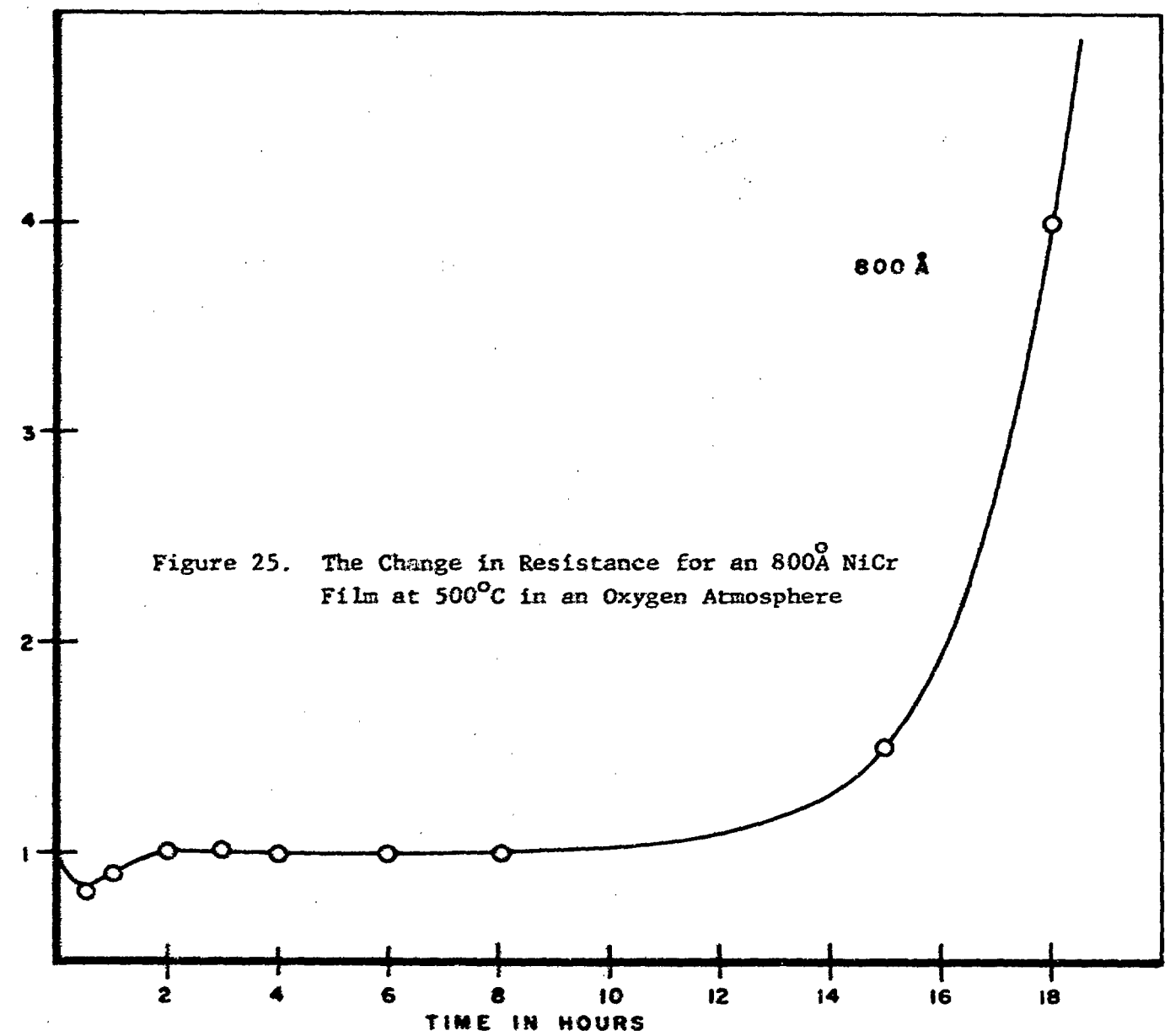

Figure 25. The Change in Resistance for an 800Å NiCr Film at 500°C in an Oxygen Atmosphere

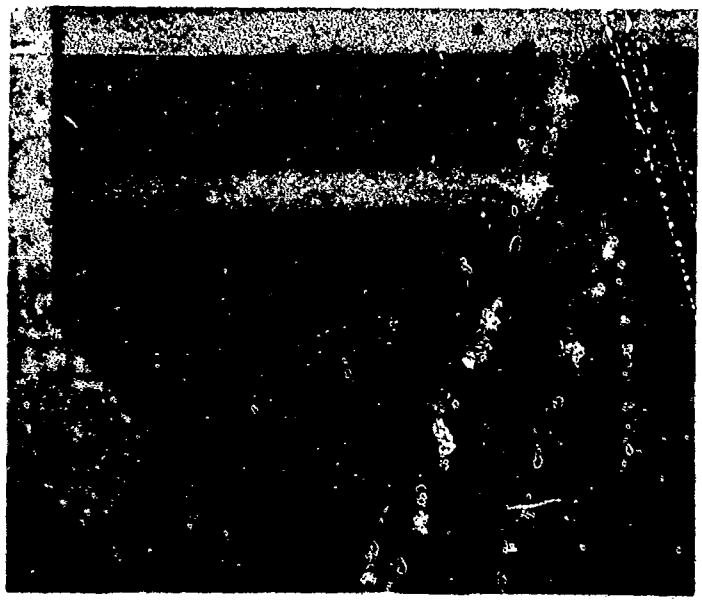

Figure 26. A NiCr Resistor Showing Spots Due to Nonuniform Oxidation (520X)

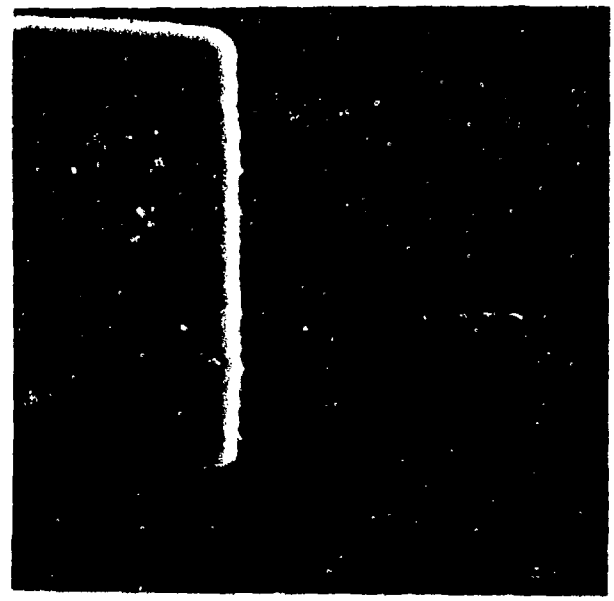

Figure 27. A Secondary Electron Image of a NiCr Resistor and Al Bonding Pad (1800X)

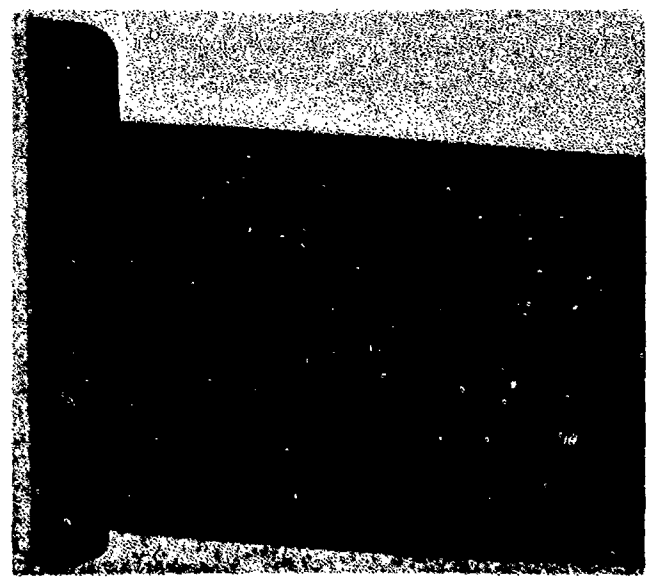

Figure 28. The EBIC Image of the Resistor Shown in Figure 27 (2100X)

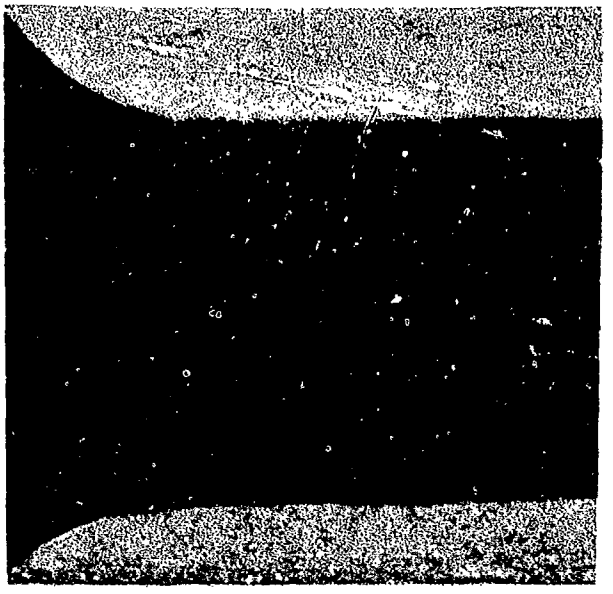

Figure 29. An EBIC Image of an As-Deposited NiCr Resistor (5000X)

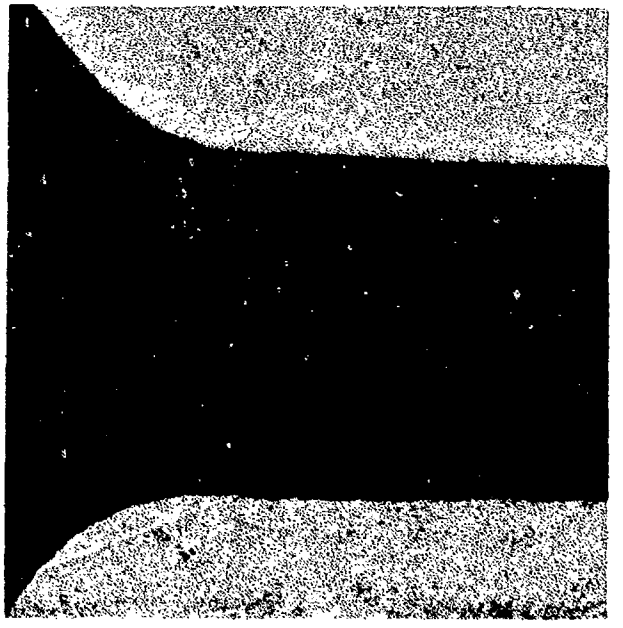

Figure 30. An EBIC Image of an NiCr Resistor that was Oxidized at 500°C for 1 Hour Showing Two Phases (4400X)

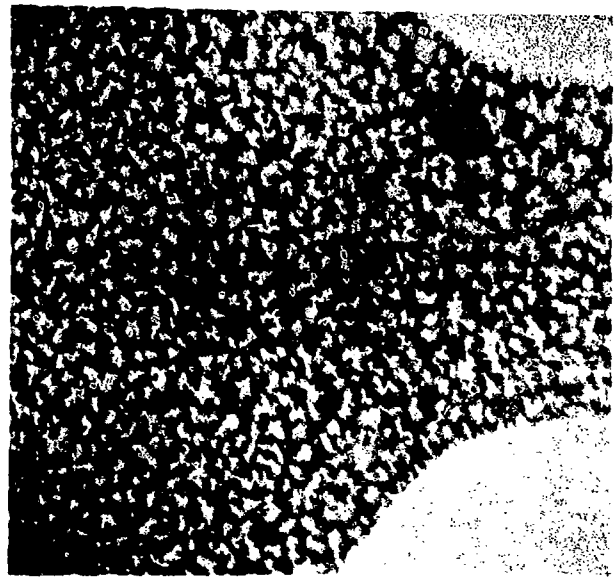

Figure 31. The EBIC Image of a Heavily Oxidized NiCr Resistor Showing a Dark Matrix with Light Colored Particles (7000X)

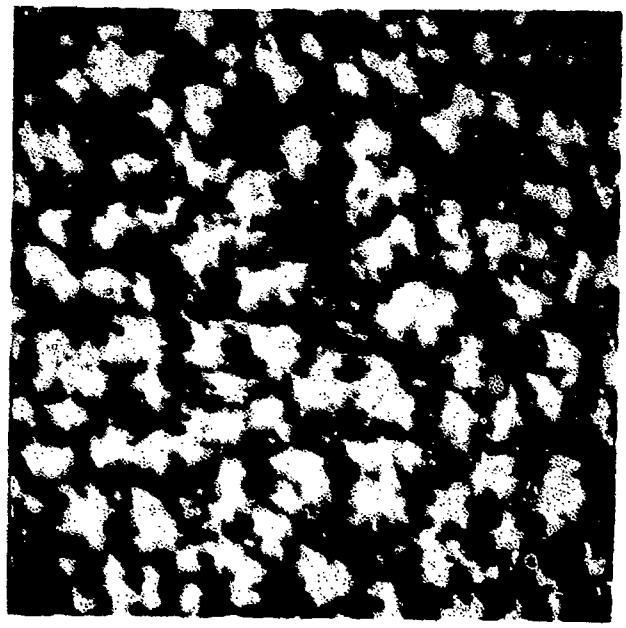

Figure 32. The Resistor of Figure 31 Showing Particles with Diameters Between 1000 and 5000Å (22,000X)

composition differences between the two regions could be measured with the multi-channel analyzer. Figure 33 is a different section of the resistor and the corresponding line scan is given in Figure 34. This scan represents the transmitted intensity; on the right is the smooth trace from the thermal oxide. The left-hand portion is the oxidized NiCr and is indicative of a rough surface. This may correspond to the thickness differences between the two phases that were observed. For a comparison with the oxidized NiCr, a resistor that was vacuum annealed at 500°C for 3 hours is shown in Figure 35, using the EBIC mode. There is no visible microstructure in this film even though the resistance had decreased by 25 percent. (The black spots in Figure 35 are due to surface contamination.) Therefore, the observed contrast is due to the oxidation.

The observed resistance changes are caused by a combination of the following processes: Precipitation, grain growth, oxidation and interdiffusion. The precipatation and grain growth lower the resistance of the nichrome as was observed in the vacuum annealed specimens. The oxidation increases the resistance by decreasing the amount of conductive material. The combination of these effects gives rise to the curves in Figures 23, 24, and 25.

The oxidation behavior is indicative of a two-step process. First, there is a rapid resistance increase caused by surface and grain boundary oxidation, and is observed at all temperatures (Figure 23). Furthermore, since the grain size is uniform, there would be proportionately more grain boundary area on the narrower resistors. Hence, they would oxidize faster than the wider resistors, as was observed in the present experiments. This oxide layer would have an effective thickness on the order of 100Å. The second step is a region where the oxidation kinetics are diffusion limited. During this time the resistance changes would be considerably slower, which accounts for plateaus in Figures 23 and 24 From bulk oxidation experiments, Kubaschewski and Hopkins[25] have given the activation energies for the diffusion of metal atoms

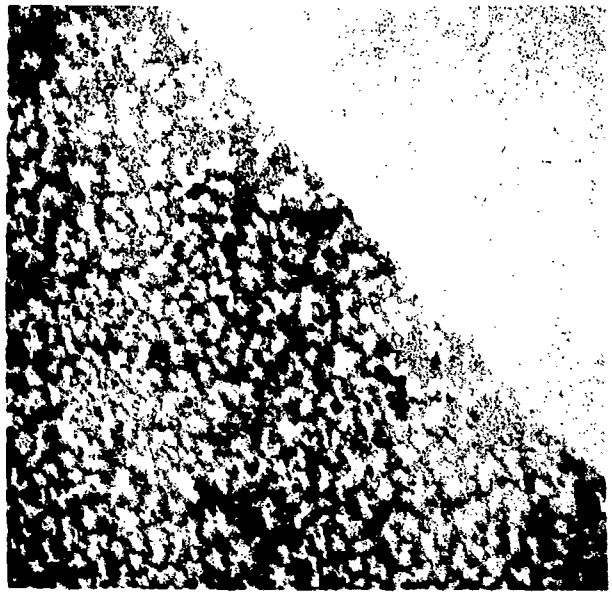

Figure 33. The EBIC Image of the Oxidized NiCr Resistor Shown in Figure 31

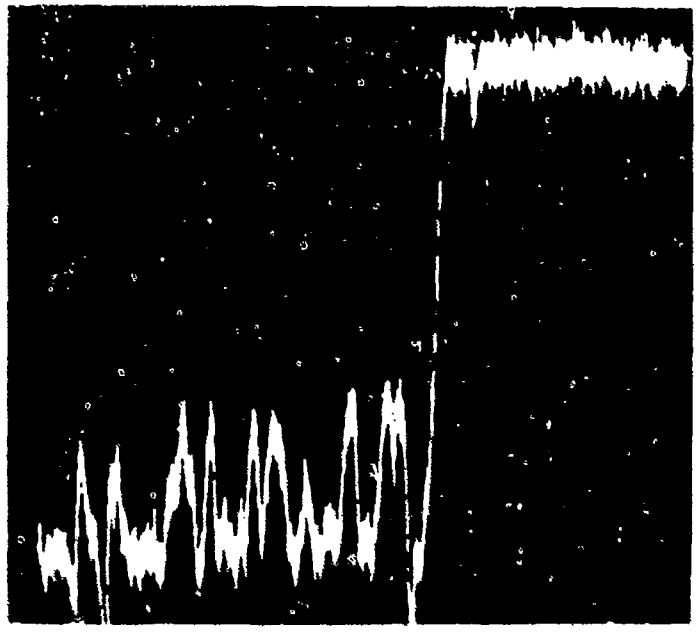

Figure 34. A Line Scan Across the Center of Figure 33 Representing the Transmitted Intensity. On the right is the smooth trace from the thermal SiO_2; on the left is the rougher trace from the oxidized NiCr.

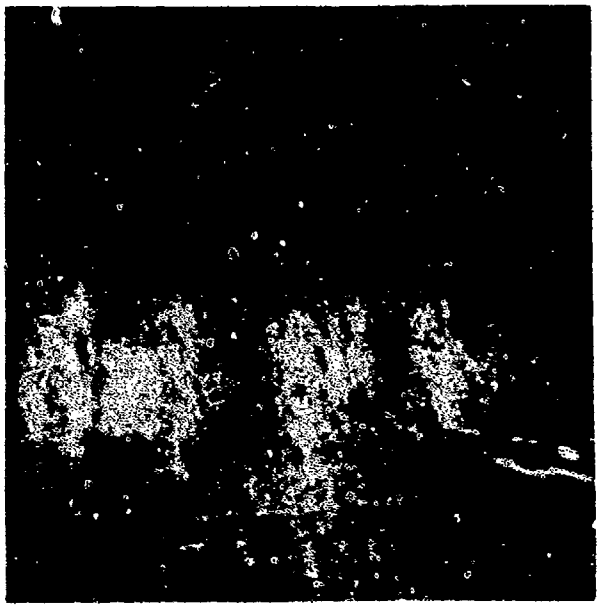

Figure 35. An EBIC Image of a Vacuum Annealed NiCr Resistor. No microstructure was visible in this film. (20,000X)

through the corresponding oxide. They are listed in Table II. The activation energy for Cr is nearly twice that for Ni through their respective oxides. Therefore, the Cr-rich nichrome should be much more oxidation-resistant than for the Ni-rich nichrome resistors. This is in agreement with the results shown in Figure 36.

The oxidation of NiCr thin films is nonuniform as was shown by the use of the EBIC mode of the SEM. Since the resistors consisted of Ni-70% Cr, local composition differences could account for the observed two phases. The oxidation kinetics[25] for bulk Ni and Cr are

$$k\ (Ni\ 0) = 8 \times 10^{-4} \exp\ (-41{,}200/RT)$$

and $$k\ (Cr_2O_3) = 3 \times 10^{-6} \exp\ (-37{,}500/RT).$$

The calculated rates in the temperature range 400 to 500°C are almost identical, so that the oxides should grow to the same thickness. The oxidation rates are given in units of $(g/cm^2)^2$, which is the same units as the product ρX. Therefore, differences in the composition and the resulting oxides would not account for the two phases observed with the EBIC technique.

Another factor which may account for the EBIC results is the effect of grain orientation on the oxidation kinetics. For Ni single crystals, the kinetics increase in the following sequence[26]: (111), (100), (211), high angle planes such as (115) and (310). This difference in oxide growth rate would result in thickness differences on the NiCr films and could account for the two-phase contrast in Figures 31 and 32 and the surface roughness observed in the line scan (Figure 34).

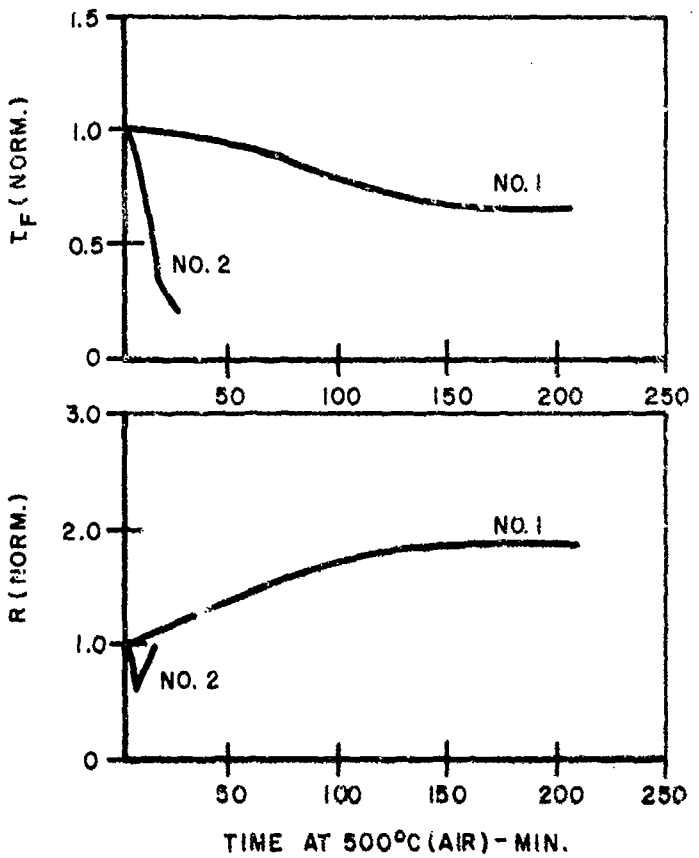

Figure 36. The Effect of Composition on the Aging of NiCr Resistors. No. 1, Ni-70Cr; No. 2, Ni-32Cr.

TABLE II

Diffusion in Metal-Oxide Systems[25]

	D_0(cm^2/sec)	Q(kcal/mole)
Ni in NiO	0.017	56
Cr in Cr_2O_3	4000	100
Ni in $NiCr_2O_4$	0.85	74.5
Cr in $NiCr_2O_4$	0.74	72.3
O in $NiCr_2O_4$	0.017	65.4

SECTION V

5.0 DIFFUSION

The presence of an Al-NiCr interface and the high temperatures encountered during circuit processing can lead to interdiffusion and the growth of intermetallic phases. Large regions of intermetallic phases can be formed by the use of bulk diffusion couples and subsequently identified by means of microprobe analysis. The kinetics of the diffusion process can be determined from thin film diffusion couples. From this data the effects of time and temperature on the reliability of NiCr resistors can be determined. In this section the diffusion data from the present experiments are presented and discussed.

Bulk diffusion couples were made by hot pressing 0.25-inch rods of Al against Ni-Cr alloys. Couples were made using three different compositions of nichrome: Ni-20% Cr, Ni-30% Cr and Ni-70% Cr. These diffusion couples were then annealed in an argon atmosphere at 550°C for various time intervals. The couples were then polished and the resulting intermetallic phases can be seen in Figures 37, 38 and 39. For the couple Al-Ni-20% Cr at least two phases are visible (Figure 37). Microprobe data for this couple yields the following phases, starting from the NiCr end: 21%Cr, 79%Ni; 13.4%Cr, 45%Ni, 41.6%Al; 11.1%Cr, 41.0%Ni, 47.9%Al; 8.1%Cr, 29.4%Ni, 62.5%Al; 1.4%Cr, 32.1%Ni, 66.5%Al; 100%Al. No microprobe data was obtained for the Ni-30Cr and Al couple. However, for the couple Ni-70Cr and Al (Figure 39), the microprobe gives compositions for the intermetallics as followed: 73.3%Cr, 26.7%Ni; 15.8%Cr, 4.1%Ni, 80.1%Al; 0.2%Cr, 1.8%Ni, 98%Al; 0.1%Cr, 8.2%Ni, 91.7%Al; 0.1%Cr, 0.14%Ni, 99.76%Al; 100%Al.

A back scatter electron image of this Ni-70%Cr-Al diffusion couple (Figure 39) is shown in Figure 40. The light-colored bands in the center of the figure have higher Ni contents then the

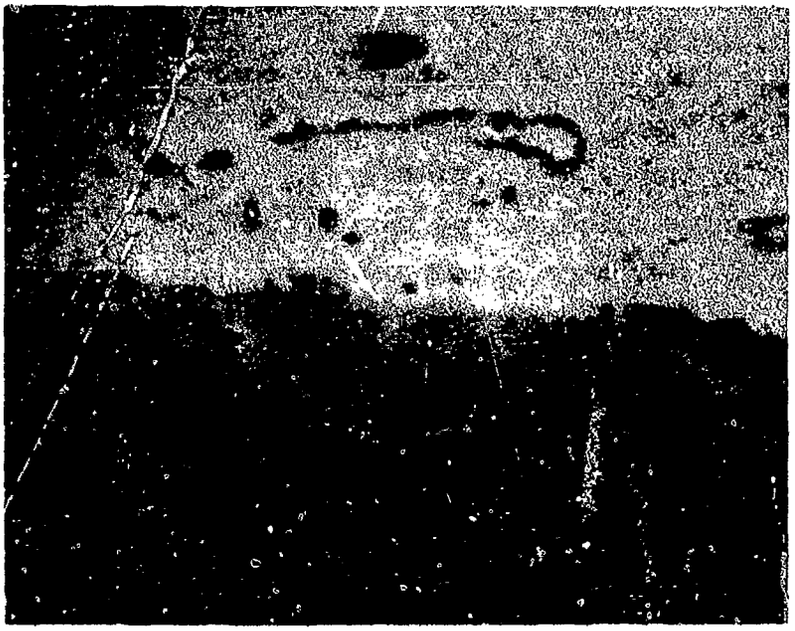

Figure 37. Diffusion Couple of Cr-80Ni and Al after 64 Hours at 550°C. Aluminum is at the bottom. (400X)

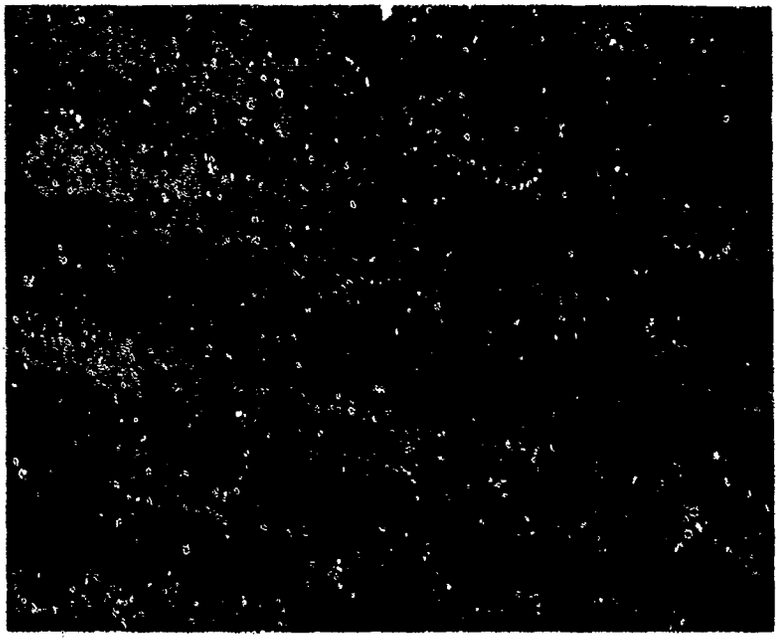

Figure 38. Diffusion Couple of Cr-70Ni and Al after 24 Hours at 550°C. Aluminum is at the bottom. (520X)

Figure 39. Diffusion Couple of Ni-70% Cr and Al After 64 Hours at 550°C. Al is at the bottom and NiCr at the top with four intermetallic regions in between (270X)

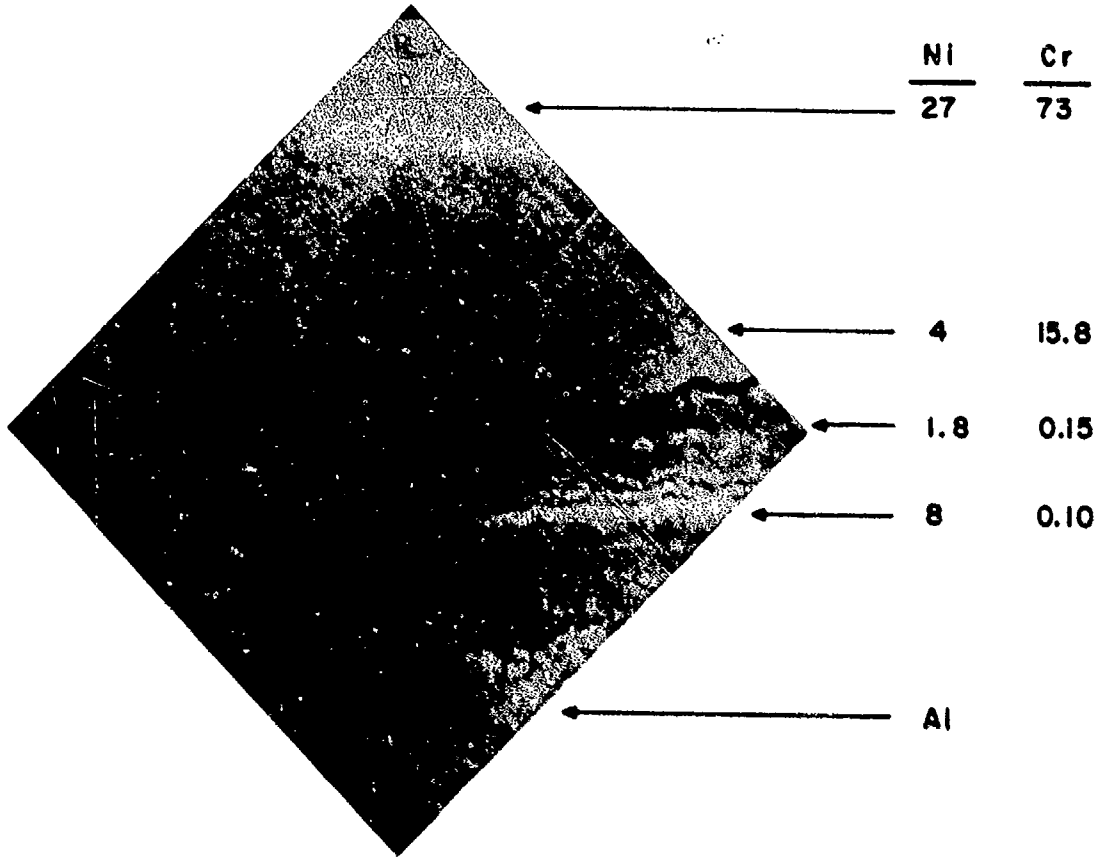

Figure 40. Backscatter Electron Image of the Diffusion Couple in Figure 39. Bands with higher Ni content are evident midway between the Nichrome and Al

adjacent regions. As can be seen from the photomicrographs and the microprobe data, the observed intermetallic phases depend upon the composition of the NiCr in contact with the Al.

The Ni-Cr-Al ternary phase diagram is shown in Figure 41. The Ni-rich corner has been determined by Taylor and Floyd[27] while the rest of the diagram has not yet been determined. The phases that were determined from the two diffusion couples are indicated on the diagram. The phases for the Ni-20%Cr-Al couple are indicated by the Arabic numbers. The first two phases (2 and 3) may correspond to the compound NiAl with Cr additions, while the other phases (4 and 5) are close to the binary compounds Ni_2Al_3 and $NiAl_3$. By comparison, the Ni-70%Cr-Al couple consists of very Al-rich compounds (B, C, D and E). The latter compounds are the ones of interest since the composition of the resistor films is Ni-70%Cr. Therefore, for the present nichrome resistors only the very Al-rich compounds will form.

The kinetics for the interdiffusion of NiCr and Al can be obtained by the annealing of resistor test patterns with Al metallization. Figure 42 shows the resulting appearance of the resistors after various annealing times at 500°C. The Al diffuses into the NiCr and also forms intermetallic phases, as seen in the films annealed for 16 hours. From these photomicrographs the penetration distance of the Al into the NiCr was obtained as a function of time. A representative plot of X^2 versus t at 525°C is shown in Figure 43, where X is the penetration distance. Since X^2 is a linear function of t, it was assumed that the diffusion can be described by the equation

$$X^2 = Dt.$$

Therefore, the slopes of the penetration plots will give the diffusion coefficients that are listed below:

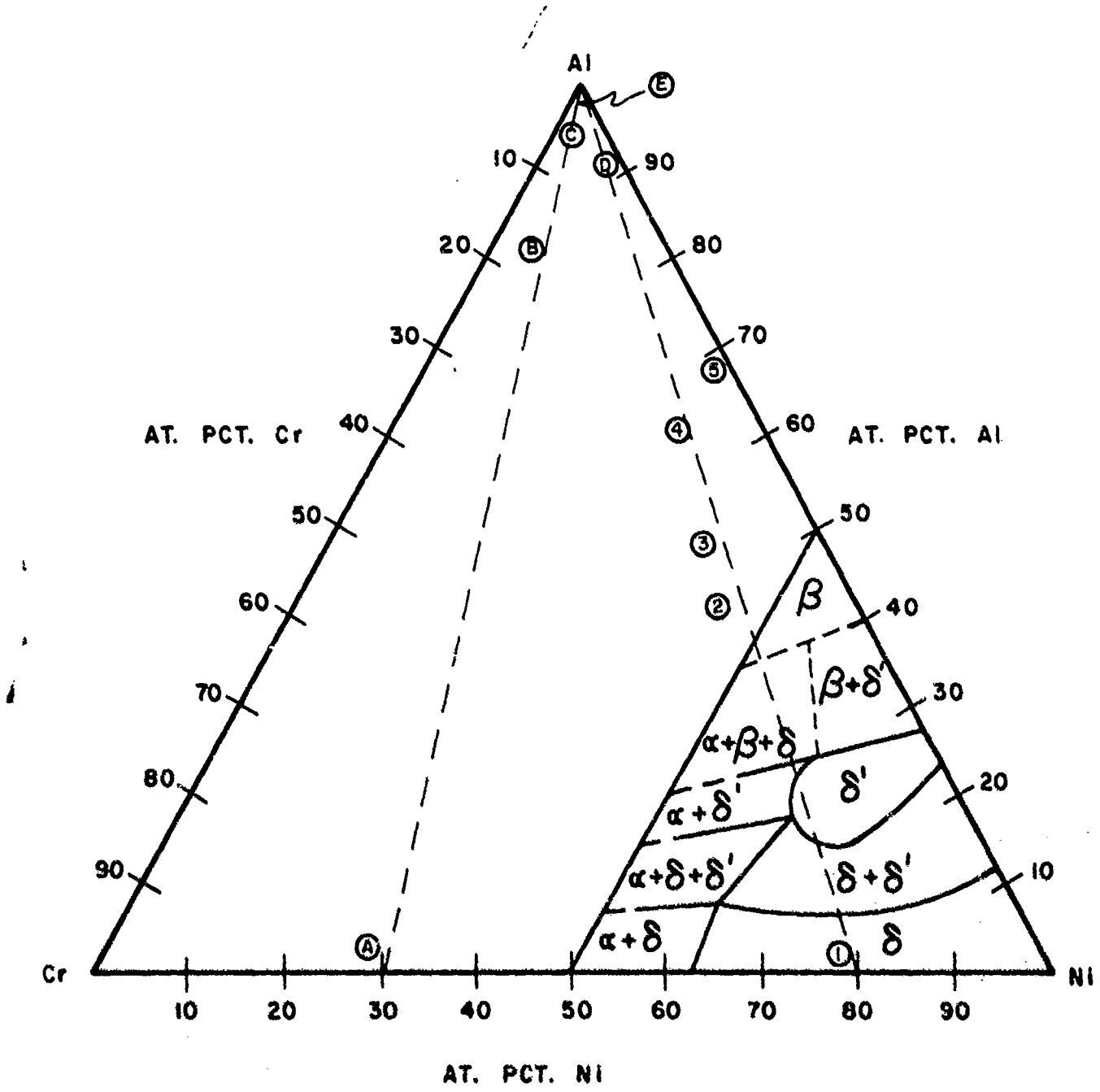

Figure 41. The Ni-Cr-Al Ternary Diagram. The Ni-rich corner was determined by Taylor and Floyd[27]. The dotted lines indicate the two diffusion couples that were run and circled numbers and letters indicate the observed phases.

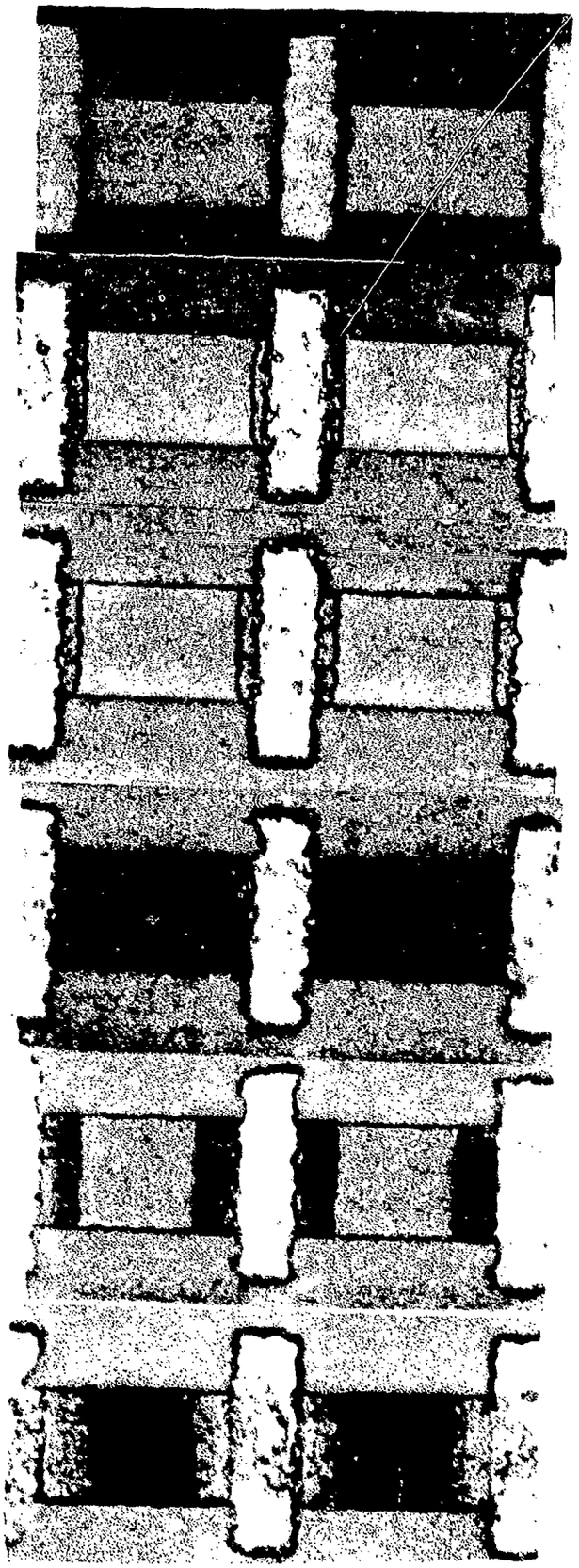

Figure 42. The Diffusion of Al into NiCr at 500°C (680X)

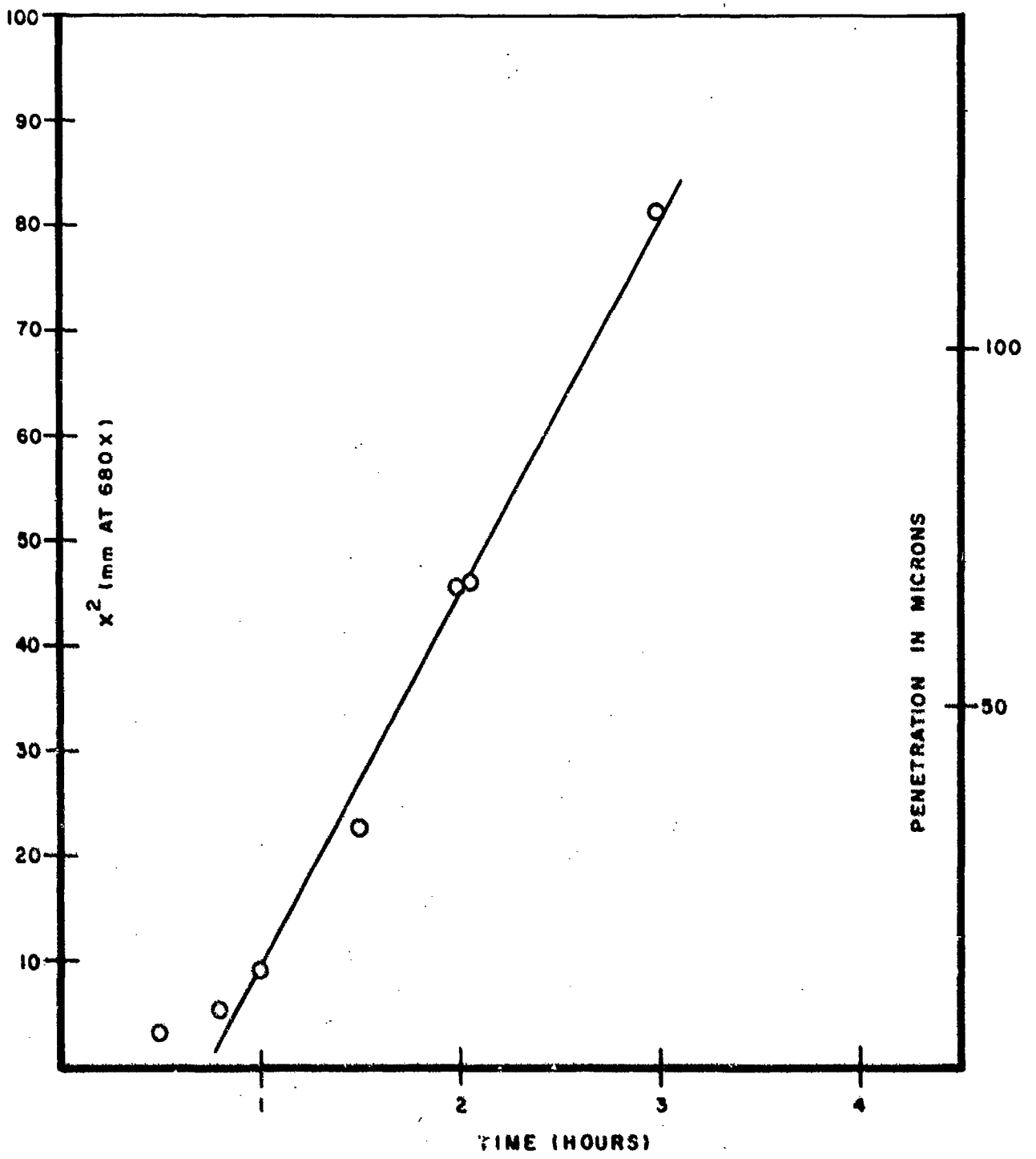

Figure 43. A Plot of X^2 Versus t for the Penetration of Al into NiCr at 525°C

T(°C)	D (cm^2/sec)
525	2.09×10^{-9}
500	1.17×10^{-10}
475	1.48×10^{-11}

An Arrhenius plot of the diffusion data is shown in Figure 44. Assuming the relationship

$$D = D_o \exp(-Q/RT),$$

an activation energy of 96 $\pm$ 30 kcal/mole was determined. The pre-exponential term D_o was on the order of 10^{16} cm^2/sec. An extrapolation of this diffusion data to lower temperatures will provide estimates of the times at fixed temperatures required for interdiffusion to a distance X. Table III presents the times required for the interdiffusion of 200Å and 1000Å NiCr films. From this table it can be seen that the normal processing temperatures and times are sufficient to form intermetallic phases at the NiCr-Al interface. However, negligible diffusion of the intermetallic into the NiCr should occur with the present process.

The diffusion kinetics for Al and NiCr thin films can be compared with those obtained using bulk alloys. The activation energies[28] for the self-diffusion of Al, Ni and Cr are 34, 69.5 and 81 kcal/mole, respectively. By comparison, the activation energy[29, 30] for the tracer diffusion of Ni^* in Al is 15.7 kcal/mole while that for Cr^* in Al is 58 kcal/mole. Askil[31] studied the diffusion of Cr^{58} in Ni-Cr alloys and found that the activation energy increases with increasing Cr contents. At a composition of Cr-20%Ni the activation energy is 62 kcal/mole. For the present experiments, the measured activation energy represents both the diffusion of the individual species and the

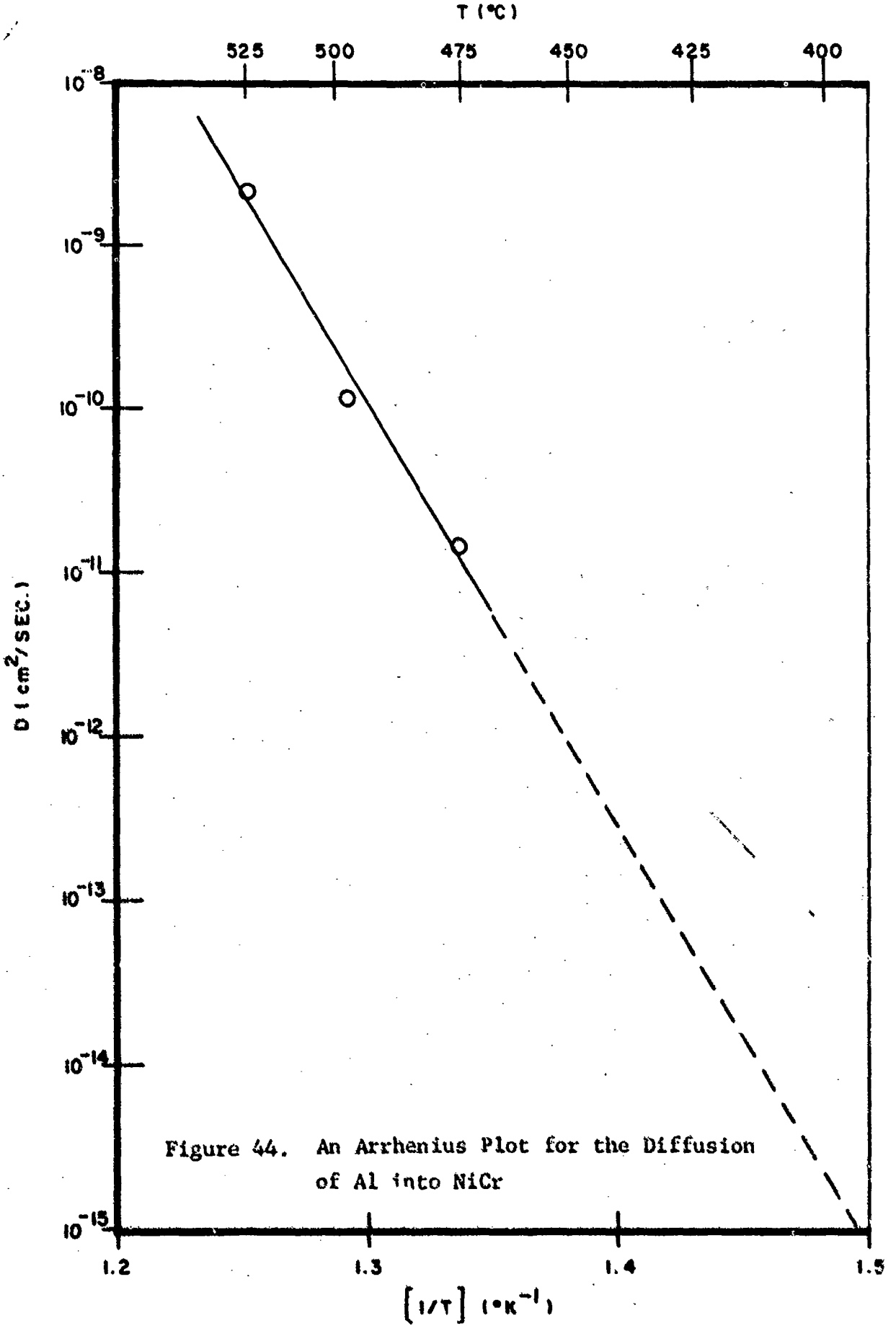

Figure 44. An Arrhenius Plot for the Diffusion of Al into NiCr

Table III

The Times Required for the Diffusion of
Al into 200Å and 1000Å of NiCr

T(°C)	distances (A)	time
400	200	33 min
	1000	14 hours
450	200	4 sec
	1000	100 sec
500	200	0.04 sec
	1000	1 sec

formation of the intermetallic compounds. Since the measured activation energy (100 kcal/mole) is considerably higher than that for tracer diffusion, the rate-limiting step is probably the formation of the intermetallic compounds rather than diffusion.

The diffusion and intermetallic phase formation should not affect the reliability of NiCr resistors. The resistance was monitored after each diffusion anneal. No large resistance changes nor discontinuities were observed even at the longest times at each temperature. These time and temperature treatments greatly exceed any combination of processing treatments. The Al-NiCr interface was also examined in the SEM. Figure 45 shows the interface after 30 minutes at 500°C; there is no indication of diffusion at a magnification of 5000X. After 3 hours at 500°C, the intermetallic phases are visible in Figures 46 and 47. These photomicrographs show a volume increase as the Al diffuses into the NiCr. Figure 48 reveals the intermetallic phases after 24 hours at 500°C. Small depressions in the Al are visible which reveal the areas from which the Al has diffused.

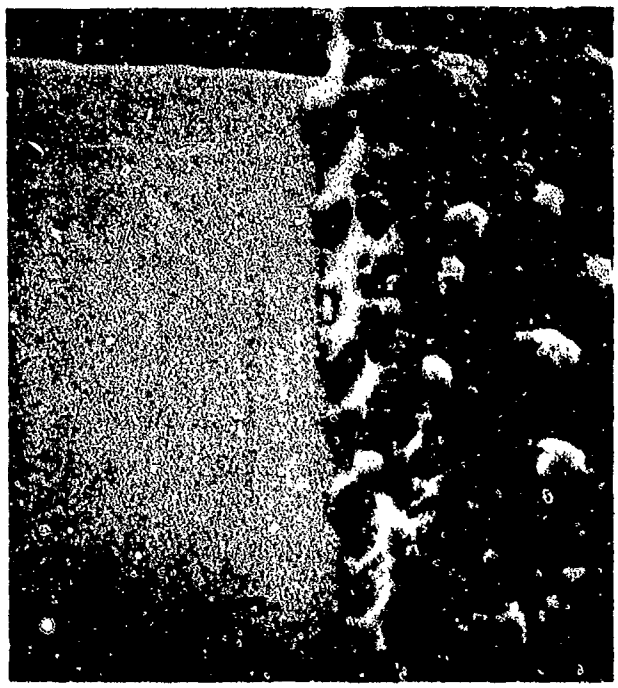

Figure 45. The Al-NiCr Interface After 30 Minutes at 500°C. (5000X)

Figure 46. The Al-NiCr Interface Showing Intermetallic Formation after 3 Hours at 500°C (5000X)

Figure 47. Another Al-NiCr Interface Showing the Intermetallic Phase and the Volume Change that Occurs

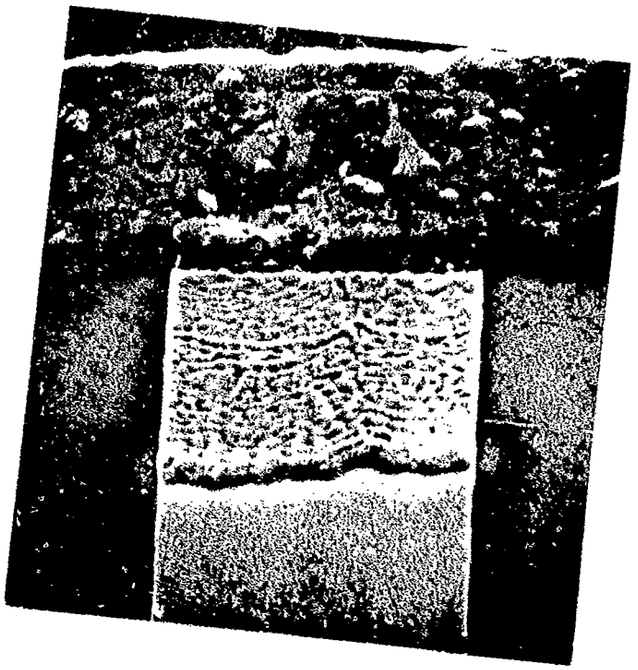

Figure 48. The Al-NiCr Interface After 24 Hours at 500°C. At least two different intermetallic phases can be seen (2000X)

SECTION VI

6.0 TEMPERATURE CYCLING TESTS

Nichrome resistors were prepared using the 98R test pattern. The composition was Ni-70%Cr and with a thickness of 180Å. The resistors were trimmed for 10 minutes at 475°C and then passivated with 10,000Å of SiO_2. The circuits were die-bonded using gold-silicon eutectic solder into ceramic flat packs which were subsequently sealed in an oxygen atmosphere. The wire bonding was performed using 1-mil Al wire; six resistors with values between 60 and 8K ohms were available for testing. The circuit diagram that was used for this test is shown in Figure 49. A current of 5mA was passed through resistors R1 through R5. No power was applied to R6 in order to separate the effects of power and temperature. The voltages at the positive ends of each resistor are as follows: R1 - 0.33V, R2 - 9.7V, R3 - 38.7V, R4 - 19.5V, R5 - 19.2V. Therefore there is sufficient voltage to cause anodic dissolution of the NiCr if moisture were available to the nichrome.

Fifty test circuits were then subjected to a temperature cycling test which consisted of the following:

(1) The temperature was raised to 125°C and maintained for 3 hours.

(2) The temperature was decreased to -55°C and maintained for 3 hours. During this time the devices were power cycled with 2.5 minutes on and 2.5 minutes off. The transfer time between temperatures was approximately 5 minutes.

(3) The devices were then allowed to slowly warm up to room temperature while the power cycling was continued at the same 5-minute rate.

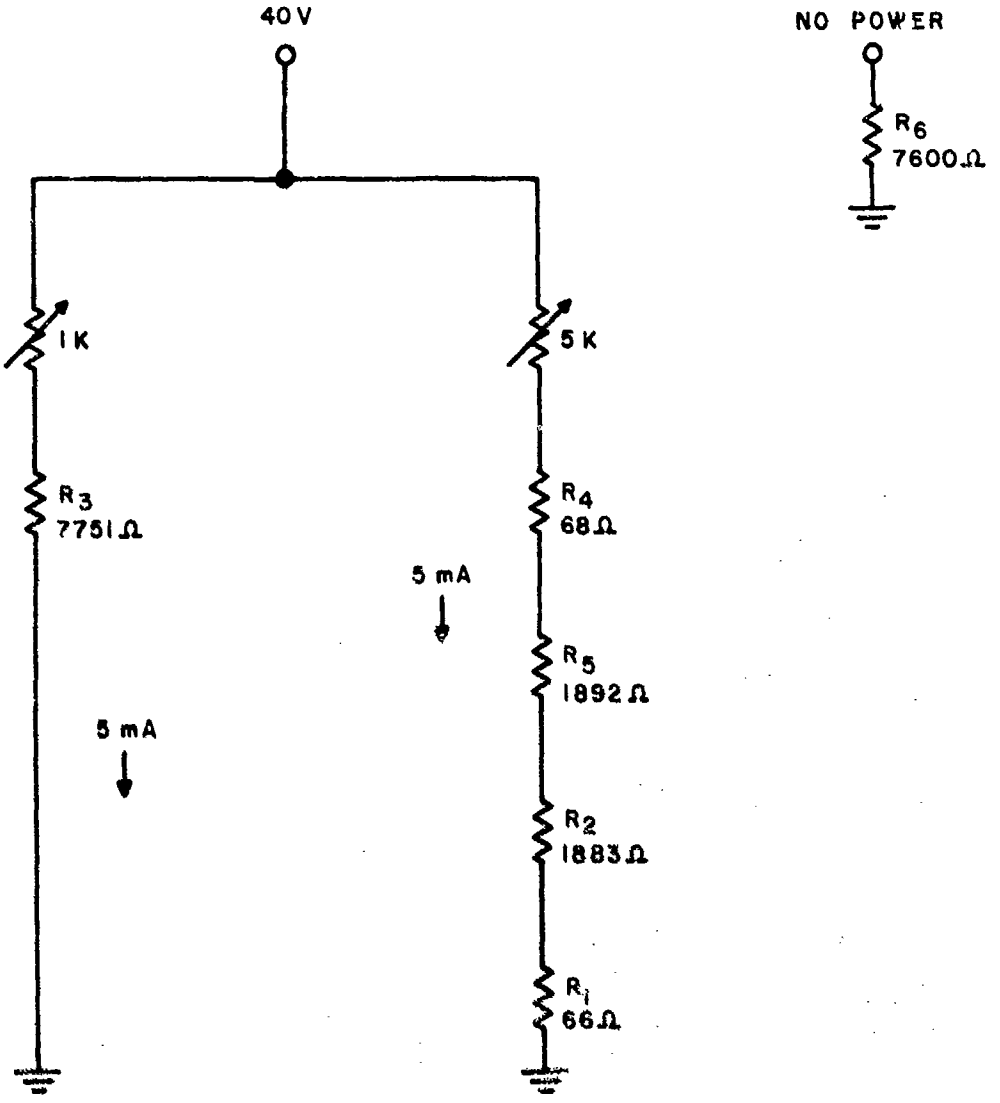

Figure 49. Circuit Diagram Used for the Temperature Cycling Test

After one temperature cycle there were no resistor failures so the test was extended for five more cycles. Again there were no resistor failures. A modification of the test was made in order to accelerate the temperature cycling. This modified temperature cycling test consisted of the following:

(1) A temperature of 125°C was maintained for 6 hours.

(2) During a 1-hour period the devices were transferred to -65°C.

(3) The temperature of -65°C was maintained for 4 hours while power cycling at a 3-minute rate.

(4) The devices were transferred over a 1-hour period to 125°C while continuing the power cycling. This cycle was then repeated.

After 25 cycles of the modified temperature cycle test using the same circuits, there were still no resistor failures. Typical resistor values for two circuits are given in Table IV. The resistor values seem to be decreasing slightly but the changes are small. It was concluded that this temperature cycling test had a negligible effect on the nichrome resistors. Therefore, the conditions under which corrosion occurs were not met during this test.

TABLE IV

Representative Values for NiCr Resistors that Were Temperature Cycled Between +125°C and -65°C With a Bias Applied at the Low Temperatures

Device No.	R1	R2	R3	R4	R5	R6
#675						
Initial	66.1	1883	7751	68.0	1892	7644
1 Cycle	62.8	1877	7754	70.0	1889	7643
6 Cycles	63.3	1873	7750	71.0	1891	7639
32 Cycles	65.3	1860	7712	63.0	1875	7602
#690						
Initial	73.8	2072	8560	74.0	2076	8490
1 Cycle	70.8	2063	8560	77.0	2070	8448
6 Cycles	70.0	2065	8550	74.0	2069	8480
32 Cycles	71.8	2050	8497	67.0	2055	8425

SECTION VII

7.0 CONCLUSIONS

The production of reliable nichrome resistors depends upon understanding and controlling a variety of different parameters. To obtain a reproducible resistance and TCR, one must control the composition, thickness, deposition processes, subsequent heat treatments, and the photoresist and delineation processes. The Cr-rich nichrome was found to be quite oxidation-resistant From the resistance measurements it was concluded that an initial oxide layer forms rapidly to approximately 100Å; the oxidation kinetics then slow down and become diffusion limited. Therefore, oxidation-resistant NiCr thin films should be deposited at thicknesses that are significantly thicker than 100Å. The subsequent oxidation adjusts the sheet resistance and the TCR and, in addition, forms a stable oxide on the surface. This stabilizes the NiCr during later processing steps involving high-temperature, oxidizing atmospheres. Furthermore, the oxidation should be performed at temperatures greater than those encountered during later processing. This should eliminate any reliability problems associated with oxidation.

The interdiffusion of the Al and the 200Å NiCr films occurs during the temperatures encountered during the present process. However, from SEM examination, times greater than 30 minutes at 500°C are necessary in order to observe diffusion at the Al-NiCr interface. Also the thermal oxidation of the NiCr will retard the diffusion kinetics. Since no resistance changes as a result of interdiffusion were observed, there should be no reliability problems caused by interdiffusion.

Nichrome thin films were found to be resistant to most of the chemicals examined with the exception of strong acids and known NiCr etches. Nichrome is subject to anodic dissolution as

are all metals. The anodic dissolution of the NiCr occurs in the presence of water at potential differences greater than 2.5 volts. It was also determined that chemically-deposited phosphorous-doped SiO_2 passivation glass provides good protection from corrosion for the thin NiCr. Aluminum is also subject to anodic dissolution, which occurs at potential differences greater than 0.5 volt.

Temperature cycling tests over the range -65 to +125°C were performed to determine the effects on NiCr resistors. The passivated test circuits were sealed in the Motorola ceramic flat pack. No effects on the NiCr resistors were observed after 32 temperature cycles. It was therefore concluded that the combination of passivation glass and the ceramic package (and sealing process) prevented any corrosion of the NiCr. Therefore, reliable nichrome resistors with aluminum terminations can be produced if the materials and processes that are involved in their production are understood and controlled.

ACKNOWLEDGMENTS

The author would like to acknowledge K. V. Ravi and E. Philofsky for their guidance and support during this project. I would also like to thank E. Hall for the EBIC results and many helpful discussions, and H. Berg for assistance with the diffusion experiments. I am also greatful for the help of T. Gonzales, D. Kirkman, L. Millikan, A. Koblinsky and V. Rysso.

REFERENCES

1. E. Philofsky, G. Stickney and K. V. Ravi, 8th Annual Proc. Reliability Phys., Las Vegas, Nevada, April, 1970, P. 191

2. V. C. Kapfer and J.J. Bart, 10th Annual Proc. Reliability Phys., Las Vegas, Nevada, April 1972, P. 175.

3. V. C. Kapfer and J.J. Bart, Technical Report RADC-TR-72-38, GAFB, New York, 1972.

4. A. DerMarderosian, Raytheon Report IS:72:6, January 1972.

5. F. A. Shunk, Constitution of Binary Alloys, Second Supplement McGraw-Hill Book Co., New York, 1969, P. 274.

6. H. Thomas, Z. Physik 129, 219 (1951).

7. W. Koestner and P. Rocholl, Z. Metallkde 48, 485 (1957).

8. J. H. Mooij and M. deJong, J. Vacuum Sci. Techn. 9, 446 (1972).

9. E. Stern, Proc. Natl. Electron Comp. Conf. 1966, P. 233.

10. T. K. Lakshmanan, Trans. Natl. Vacuum Symp. 8, 868 (1961).

11. H. J. Degenhart and I. H. Pratt, Trans. 10th AVS Symp. (1963), P. 480.

12. D. S. Campbell and B. Hendry, Brit. J. Appl. Phys. 16, 1719 (1965).

13. R. W. Bicknell, H. Blackburn, D. S. Campbell and D. S. Stirland, Microelectronics and Reliability 3, 61 (1964).

14. T. M. Nenadovic, Z. B. Fotiric, T. S. Dimitrijeric and M. B. Adamov, Thin Solid Films 10, 45 (1972).

15. L. Maissel, "Thin Film Resistors", in Handbook of Thin Film Technology, ed. L.I. Maissel and R. Glang, McGraw-Hill Book Co. New York, 1970, Ch. 18.

16. R. W. Berry, P. M. Hall and M. T. Harris, Thin Film Technology, Van Nostrand Reinhold Co., New York, 1968. Chs. 6 and 7.

17. N. Schwartz and R. W. Berry, Physics of Thin Films 2, 363 (1971)

18. G. W. A. Dummer, Materials for Conductive and Resistive Functions, Hayden Book Co., Inc. New York, 1970.

19. J. G. Swanson & D. S. Campbell, Thin Solid Films 1, 183 (1967).

20. J. M. West, Electrodeposition and Corrosion Processes, D. Van Nostrand and Co. Ltd. 2nd Ed. London, 1970.

21. M. Pourbaix, Atlas of Electrochemical Equilibria in Aqueous Solutions, Pergamon Press, Oxford, 1966.

22. R. Glang and L. V. Gregor, "Generation of Patterns in Thin Films", in Handbook of Thin Film Technology, Ed. L.I. Maissel and R. Glang, McGraw-Hill Book Co., 1970. Ch. 7.

23. H. H. Uhlig, Corrosion and Corrosion Control, J. Wiley and Sons, Inc., New York, 1963. Ch. 22.

24. E. Hall, Technical Report ECOM-0164F, United States Army Electronics Command, Fort Monmouth, N.J., October 1971.

25. O. Kubaschewski and B. E. Hopkins, Oxidation of Metals and Alloys, Academic Press, Inc. 2nd Ed. London, 1962.

26. A. T. Gwathney and K. R. Lawless, "The Influence of Crystal Orientation on the Oxidation of Metals", in The Surface Chemistry of Metals and Semiconductors, H. C. Gatos, John Wiley & Sons, New York 1966, PP. 483-521.

27. A. Taylor and R. W. Floyd, J. Inst. Met. 81, 451 (1953).

28. C. J. Smithells, Metals Reference Book, 4th Ed. Plenum Press, New York, 1967.

29. K. Hirano, R. P. Agarwala and M. Cohen, ACTA Met. 10, 857 (1962).

30. N. L. Peterson and S. J. Rothman Phys. Rev. B1, 3264 (1970).

31. J. Askil, Phys. Stat. Sol. A8, No. 2, 587 (1971).

UNCLASSIFIED

Security Classification

DOCUMENT CONTROL DATA - R & D

(Security classification of title, body of abstract and indexing annotation must be entered when the overall report is classified)

1. ORIGINATING ACTIVITY (Corporate author)

Motorola, Incorporated
Semiconductor Products Division
5005 E. McDowell Road, Phoenix, Arizona 85005

2a. REPORT SECURITY CLASSIFICATION

UNCLASSIFIED

2b. N/A

3. REPORT TITLE

RELIABILITY OF THIN FILM NICHROME RESISTORS
USED ON RADIATION HARDENED INTEGRATED CIRCUITS

4. DESCRIPTIVE NOTES (Type of report and inclusive dates)

Final Report (19 October 1971 - 19 June 1972)

5. AUTHOR(S) (First name, middle initial, last name)

Wayne M. Paulson

6. REPORT DATE	7a. TOTAL NO. OF PAGES	7b. NO. OF REFS
April 1973	74	31

8a. CONTRACT OR GRANT NO.	9a. ORIGINATOR'S REPORT NUMBER(S)
F30602-72-C-0069 Job Order No. 88090301	None
	9b. OTHER REPORT NO(S) (Any other numbers that may be assigned this report) RADC-TR-73-105

10. DISTRIBUTION STATEMENT

Distribution limited to US Gov't agencies only; test and evaluation; April 1973. Other requests for this document must be referred to RADC (RBRM), GAFB, NY 13441.

11. SUPPLEMENTARY NOTES	12. SPONSORING MILITARY ACTIVITY
None	Rome Air Development Center (RBRM) Griffiss Air Force Base, New York 13441

13. ABSTRACT

The effects of corrosion, oxidation and interdiffusion on the reliability of thin film Ni-Cr resistors were studied. These properties were found to depend upon the composition and thickness of the films. The Ni-Cr thin films were found to be corrosion-resistant to salt solutions and to most acids with the exception of HF solutions and now Ni-Cr etches. From "water drop" tests it was found that unpassivated resistors are subject to anodic dissolution at potentials above 2.5V. The Al metallization also dissolves at potentials above 0.5V. Passivation with 10KÅ of SiO_2 protects the nichrome from anodic dissolution. The oxidation kinetics for 180 and 460Å films show an initial rapid increase in resistance followed by a slower diffusion-limited process. By comparison, the resistance for 800Å films remained nearly constant until after 8 hours at 500°C. The EBIC mode of the SEM revealed two phases in the films, so it was concluded that oxidation is a nonuniform process. Aluminum was observed to diffuse into the Ni-Cr resistors with an activation energy of 96kcal/mole. No discontinuities in resistance were observed for times up to 24 hours at 500°C.

DD FORM 1 NOV 1473

UNCLASSIFIED

Security Classification

UNCLASSIFIED

Security Classification

14. KEY WORDS	LINK A		LINK B		LINK C	
	ROLE	WT	ROLE	WT	ROLE	WT
Nichrome Resistors Radiation Hardening Reliability						

UNCLASSIFIED

Security Classification